creative commons
COMMONS DEED

저작자표시-비영리-변경금지 2.0 대한민국

이용자는 아래의 조건을 따르는 경우에 한하여 자유롭게

- 이 저작물을 복제, 배포, 전송, 전시, 공연 및 방송할 수 있습니다.

다음과 같은 조건을 따라야 합니다:

저작자표시. 귀하는 원저작자를 표시하여야 합니다.

비영리. 귀하는 이 저작물을 영리 목적으로 이용할 수 없습니다.

변경금지. 귀하는 이 저작물을 개작, 변형 또는 가공할 수 없습니다.

- 귀하는, 이 저작물의 재이용이나 배포의 경우, 이 저작물에 적용된 이용허락조건을 명확하게 나타내어야 합니다.
- 저작권자로부터 별도의 허가를 받으면 이러한 조건들은 적용되지 않습니다.

저작권법에 따른 이용자의 권리는 위의 내용에 의하여 영향을 받지 않습니다.

이것은 이용허락규약(Legal Code)을 이해하기 쉽게 요약한 것입니다.

Disclaimer

dCollection

Ph.D. DISSERTATION

Opportunistic Spatial Reuse in High-density WLANs

고밀도 무선랜 환경에서의 기회적 공간 재사용 기법

BY

LEE HYUNJOONG

FEBRUARY 2020

DEPARTMENT OF ELECTRICAL ENGINEERING AND
COMPUTER SCIENCE
COLLEGE OF ENGINEERING
SEOUL NATIONAL UNIVERSITY

Ph.D. DISSERTATION

Opportunistic Spatial Reuse in High-density WLANs

고밀도 무선랜 환경에서의 기회적 공간 재사용 기법

BY

LEE HYUNJOONG

FEBRUARY 2020

DEPARTMENT OF ELECTRICAL ENGINEERING AND
COMPUTER SCIENCE
COLLEGE OF ENGINEERING
SEOUL NATIONAL UNIVERSITY

Opportunistic Spatial Reuse in High-density WLANs

고밀도 무선랜 환경에서의 기회적 공간 재사용 기법

지도교수 박 세 웅

이 논문을 공학박사 학위논문으로 제출함

2020년 2월

서울대학교 대학원

전기 컴퓨터 공학부

이 현 중

이현중의 공학박사 학위 논문을 인준함

2020년 2월

위 원 장:	김 종 권	(인)
부위원장:	박 세 웅	(인)
위 원:	심 병 효	(인)
위 원:	오 정 석	(인)
위 원:	주 창 희	(인)

Abstract

The explosion of mobile traffic volume has led to dense deployment of IEEE 802.11 WLANs. As a consequence, interference between neighboring basic service sets (BSSs) get severe, leading to significant air-time depletion for data transmissions. In this dissertation, we propose two different algorithms to mitigate the interference between neighboring BSSs.

First, we develop an opportunistic air-time sharing scheme, named *BeaconRider*, that facilitates simultaneous data and beacon transmissions aimed at improving spectrum efficiency in dense network environments. The proposed method works for downlink communication and allows access points (APs) to coordinate with each other in a distributed manner to exploit opportunities provided by the capture effect. Our protocol is backward compatible with legacy 802.11 APs. Through experiments with a prototype implementation using off-the-shelf IEEE 802.11n dongles as well as extensive ns-3 simulation, we show that the proposed method achieves substantial performance gains that increase with the number of APs.

Second, we propose an opportunistic spatial reuse scheme, called *OSR*, that facilitates simultaneous data transmissions of two BSSs aimed at utilizing spatial reuse opportunity in IEEE 802.11ax WLANs. *OSR* provides distributed coordination between BSSs for achieving spatial reuse (SR) gain without incurring additional control overhead. Using ns-3 simulation, we demonstrate that *OSR* significantly improves network throughput by efficiently selecting SR transmission links.

keywords: beacon frame, air-time sharing, capture effect, interference mitigation, BSS color, OBSS PD, spatial reuse, high-density WLANs, IEEE 802.11ax WLANs
student number: 2012-20846

Contents

Abstract **i**

Contents **ii**

List of Tables **v**

List of Figures **vi**

1 Introduction **1**

1.1 Motivation 1

1.2 Background and Related work 2

1.2.1 Capture Effect 2

1.2.2 BSS color 3

1.2.3 Related Work 3

1.3 Contributions and Outline 6

2 *BeaconRider*: Opportunistic Sharing of Beacon Air-Time in Densely Deployed WLANs **8**

2.1 Introduction 8

2.2 Beacon congestion problem 11

2.3 Design of *BeaconRider* 13

2.3.1 Overview of *BeaconRider* 13

2.3.2 Operation of Ridee 15

2.3.3 Operation of Rider 15
2.4 Reliability of Beacon Transmission 19
2.4.1 Beacon Frame Error Rate (BFER) 19
2.4.2 Measurement-based Calculation of Beacon Reception Ratio (BRR) 21
2.4.3 Numerical Results 22
2.4.4 Beacon Loss Detection 23
2.5 Performance Evaluation 23
2.5.1 Prototype Implementation 23
2.5.2 Simulation Results 31
2.6 Summary 34

3 *OSR*: Opportunistic Spatial Reuse in IEEE 802.11ax WLANs 35
3.1 Introduction 35
3.2 OBSS PD-based Spatial Reuse 37
3.2.1 Procedures 37
3.2.2 Limitations 38
3.3 Design of *OSR* 39
3.3.1 Overview of *OSR* 40
3.3.2 Listening 41
3.3.3 SR BSS Selection 41
3.3.4 SR Transmission 42
3.4 Performance Evaluation 43
3.4.1 Simulation Setup 43
3.4.2 Simulation Results 44
3.5 Summary 46

4 Conclusion 47

Abstract (In Korean) 54

Acknowlegement **56**

List of Tables

2.1 Summary of beacon frame statistics 13

List of Figures

2.1 Example of simultaneous transmission of beacon and data frames. . . 9

2.2 Statistics of beacon frames in practical WLANs. Total 3,218 beacon frames are collected from 20 campus buildings and 14 commercial WLAN hotspots. 12

2.3 Frame structure of the IEEE 802.11 beacon frame. Marked fields are of active use under *BeaconRider* for the coordination between APs. . 14

2.4 Timeline example of riding data-ACK transmissions. 17

2.5 Example of two BSSs. Each STA is associated with the closest AP in terms of received signal strength (RSS), and the shaded area (A) is the coverage of AP1. 19

2.6 Measurements on the beacon reception ratio (BRR) according to the SIR value. Beacon frames of 280 bytes are transmitted at rate 1 Mbps. We averaged 5 measurements, and each iteration lasts for 3 minutes. The red line is obtained by interpolating experimental results. 21

2.7 Expected beacon frame error rate (BFER) according to the STA's location (x, y). The peak BFER (7.6%) is observed at line $x = d_{\mathrm{AP1,AP2}}/2$. 22

2.8 Block diagram of *BeaconRider*. 24

2.9 Floor plan. 24

2.10 Riding success ratio (RSR), throughput, and throughput gain for a single-source scenario. 25

2.11 Riding success ratio (RSR) and beacon reception ratio (BRR) for a multi-source scenario. 26
2.12 Throughput and throughput gain for a multi-source scenario. 27
2.13 Impact of MCS selection and adaptive riding (AR) on RSR and throughput. 28
2.14 Throughput of each AP under the coexistence of BAPs and legacy APs. 29
2.15 Beacon riding under partially overlapped channels. 30
2.16 7/19 BSS layout for a static topology scenario. 32
2.17 Beacon reception ratio (BRR), throughput, and number of riding trials in a static topology scenario. 33
2.18 Beacon reception ratio (BRR) and throughput in a random topology scenario. 34

3.1 Illustration of the adjustment of OBSS PD threshold. 38
3.2 HE PPDU frame format. 40
3.3 Timeline example of OSR transmission. 43
3.4 BSS layout for simulation topology. 44
3.5 Throughput for a two BSSs scenario. 45
3.6 Link selection gain for a two BSSs scenario. 45
3.7 Throughput for a multiple BSSs scenario. 46

Chapter 1

Introduction

1.1 Motivation

With the ever-increasing demand for wireless traffic and user experience, wireless local area networks (WLANs) have attracted great attention to support the demand due to its high speed, ease of deployment, and cost efficiency. As a result, WLANs have been massively deployed in various environments such as apartments, subway stations, offices, and campus buildings. Accordingly, it have allowed users to access to the internet more easily and attain higher data rates.

However, such proliferation of WLANs leads to generate multiple overlapping basic service sets (OBSSs), where severe interferences between BSSs degrade performance and throughput by limiting transmission opportunity. As the number of APs increases, the air-time for periodically transmitting beacon frames linearly increases, which reduces channel access time to transmit data frames. Besides that, data frames from one BSS causes frame errors among neighboring BSSs by deteriorating signal-to-interference-plus-noise ratio (SINR).

In order to improve the performance and enhance channel utilization in densely deployed scenarios, IEEE 802.11ax for high-efficiency WLANs (HEW) is currently being developed [1–3]. IEEE 802.11ax aims to improve network efficiency and the

average per-user throughput in dense environments, instead of increasing the physical transmission rate and peak throughput under a single-user scenario. While there are several new technical features to achieve this goal, one of the most promising techniques is spatial reuse (SR). It allows multiple APs or STAs to simultaneously transmit frames in a specific area. In spite of the benefits of SR operation, its potential is still unknown.

Our main goal in this dissertation is to develop solutions that utilizes SR operation and mitigates interferences between BSSs in high-density WLANs. To this end, we first investigate the impact of beacon frames to the network throughput and propose beacon air-time sharing scheme that activates simultaneous data and beacon transmissions. Then, we next develop an opportunistic spatial reuse scheme that enables simultaneous data transmissions.

1.2 Background and Related work

1.2.1 Capture Effect

When two nodes simultaneously transmit different frames toward the same receiver on the same channel, the both frames may be garbled due to mutual interference. In practice, however, it is often observed that one frame with considerably higher signal strength is successfully decoded at the receiver despite the interference. This phenomenon is named *capture effect* [4–6].

To trigger the capture effect and successfully receive a certain frame (say target frame), high signal-to-interference-ratio (SIR) is required at the receiver. The transmission result depends on the selected modulation and coding scheme (MCS) level of the target frame as well as the arrival order of the two frames. Let the sender denote the AP that transmits the target frame. According to the arrival order of the target frame, the conditions for the capture effect are given as follows [7].

- *Sender-first capture*: In this case, the target frame arrives first and the second frame acts as interference. For the target frame of MCS level x to be captured at the receiver, it requires that the SIR should be greater than threshold θ_x. It is known that θ_x increases with x.

- *Sender-last capture*: In this case, the target frame arrives later. The receiver has already started decoding the first frame when the target frame arrives. It can detect the target frame only when the SIR is greater than ψ. This value is often denoted as *capture threshold* and known to be 10 dB for *ath9k* chipsets [7]. After the receiver detects the target frame, it is necessary for the SIR to be greater than θ_x again for successful decoding of data transmitted with MCS level x. As a result, we have the SIR threshold for the sender-last capture of MCS level x as $\max\{\theta_x, \psi\}$.

1.2.2 BSS color

BSS color is an identifier of the BSS. By using this, the AP or STA can easily distinguish whether the received frame transmitted from the intra-BSS (i.e., own BSS) or inter-BSS (i.e., other BSS). The BSS color is determined by the AP and is announced in the preamble of Wi-Fi frames. Specifically, the BSS color, which is a value in the range of 1 to 63, is included in the *HE-SIG-A* field in HE physical protocol data unit (PPDU). If BSS color collision occurs (i.e., two different BSSs uses the same BSS color), an HE AP selects a new BSS color and announce it to the associated STAs by sending one of beacon, probe response, and reassociation response frames.

1.2.3 Related Work

We summarize previous works in beacon congestion mitigation, air-time sharing, and SR operation relevant to *BeaconRider* and *OSR*.

Beacon congestion mitigation

There have been many efforts that aim to address the air-time depletion problem due to excessive beacon frames. A direct approach is to adjust the beacon interval to reduce beacon congestion [8–10]. In [8], the authors propose using double hundred beacon interval (2HKBI) for opportunistic device-to-device communication to reduce energy consumption and bandwidth overhead. For wireless HTTP clients, a dynamic beacon interval adaptation method based on round-trip time (RTT) is proposed [9]. In [10], an AP adjusts the beacon interval according to client traffic. However, an enlarged beacon interval induces longer delay for power save mode (PSM) enabled devices, thus it is not suitable for latency-sensitive traffic or real-time applications such as VoIP applications.

Instead of changing the beacon interval, air-time for beacon transmissions can be reduced by increasing transmission rate [11, 12]. A beacon congestion control algorithm that adjusts beacon transmission rate for vehicular ad-hoc networks is proposed in [11]. A beacon transmission rate control algorithm for cooperative vehicular networks is advanced in [12]. Changing beacon transmission rate is not backward compatible, a key feature of *BeaconRider*.

A third class of methods aims to mitigate interference from beacon transmissions through power management [13–15]. In [13], a method for adjusting beacon transmission power based on traffic forecast is proposed. Beacon transmission power control that reduces collision rate under high beacon load is advanced in [14, 15]. Both beacon transmission rate and power control affect the transmission range of APs. Time-varying coverage may also lead to frequent deauthentication of boundary STAs. Beacon interval, transmission rate, and power adjustment are control dimensions complementary to our approach of exploiting capture effect for simultaneous data and beacon transmissions.

Air-time sharing

Several studies have targeted spectrum efficiency by allowing simultaneous transmission through scheduled air-time [5, 16, 17]. In [5], the authors propose a MAC frame scheduler called *Shuffle* that coordinates frame transmission orders and supports simultaneous transmission from multiple APs. In [16], a fine-grained network coordination called *CENTAUR* that centrally schedules hidden and exposed terminals is presented. Both *Shuffle* and *CENTAUR* require a centralized controller to maintain precise time synchronization across multiple APs. From a deployability perspective, these approaches are limited in WLANs that are part of a single administrative domain. In [17], the authors propose a distributed protocol, *CMAP*, that constructs a conflict map and supports simultaneous transmission from multiple exposed terminals. This requires modifications at the MAC frame structure that does not warrant backward compatibility. In [18], the authors propose an opportunistic concurrent transmission protocol called *DOMCT* which exploits capture effect in a distributed manner. *DOMCT* requires STA's SINR feedback to construct interference map which makes it difficult to deploy the proposed algorithm in real environments.

There have been efforts to recover collided frames after simultaneous transmission by using data coding techniques [19–21]. Although these techniques can provide significant throughput improvement in interference prone WLANs, they require changes at both AP and STAs, and do not provide backward compatibility. Our technique can coexist with most of these coding techniques, resulting in further performance improvement.

Air-time sharing in heterogeneous Bluetooth and WLAN has been studied in [22, 23]. The authors in [22] and [23] have shown that a dual-stack device with Bluetooth and WLAN modules can opportunistically improve spectral efficiency of one protocol using the other's unused periods. Our approach falls in the air-time sharing category that exploits capture effect to facilitate simultaneous beacon and data transmissions in a backward compatible manner without requiring centralized control.

Spatial reuse

There are many studies have investigated the effects of carrier sensing threshold (CST) control and transmission power control (TPC) on SR operation for IEEE 802.11ax networks. In [24], a dynamic sensitivity control algorithm called *DSC* was first proposed and further evaluated in [25, 26]. *DSC* dynamically adjust the CST based on the average received signal strength (RSS) of beacon frames. However, *DSC* only considers CST control without exploiting TPC for further performance improvement. Based on the OBSS packet detection (OBSS PD)-based SR operation, the authors in [27] propose a control OBSS PD sensitivity threshold algorithm, named *COST*, that adjusts OBSS-PD threshold based on the interference level observed and the RSS from the associated STAs. In [28], the authors develop *RTOT* that uses beacon RSS to dynamically compute CST and controls transmission power based on the CST value. However, both [27, 28] do not consider the impact of the SR transmission on the ongoing transmission.

1.3 Contributions and Outline

In this dissertation, we mitigate the air-time shortage problem due to the interference between neighboring BSSs in high-density WLANs. To achieve this goal, we opportunistically utilize SR opportunity to improve channel access efficiency and network throughput. Based on the prototype implementation and extensive simulations, we demonstrate that our proposed solutions can significantly enhance network performance.

This dissertation is organized as follows. In Chapter 2, we focus on the problem of air-time depletion due to beacon transmissions which are essential for the operation of a BSS. By conducting extensive measurement study, we confirm that up to 43.9% can be taken up by beacon frames, which leads to significant reduction of air-time for data transmissions. To address the air-time depletion problem, we introduce a new

approach of air-time sharing called *BeaconRider* that allows simultaneous data transmission during the air-time of beacon transmission of neighboring APs. To this end, we develop a distributed protocol that explicitly exploits the capture effect based on real-world measurement characteristics and coordinates air-time sharing in an efficient and reliable manner. The protocol selects two appropriate APs such that the beacon frame is sufficiently protected from the interference of the data-ACK transmissions, and at the same time, data-ACK transmissions are likely to be successful under beacon interference. Through prototype implementation and extensive ns-3 simulations, we show that *BeaconRider* improves network performance with the number of deployed APs.

In Chapter 3, we focus on the IEEE 802.11ax SR operation to increase SR opportunity in dense environments. To enhance the proposed SR operation in the 802.11ax amendment called OBSS PD, we first investigate the limitations of the OBSS PD operation. Then, we propose a new algorithm called *OSR* that allows simultaneous data transmissions during the air-time of data transmission of neighboring APs. In order to accomplish this, we design a distributed protocol that schedules BSS color for initializing additional SR transmission without harming the ongoing transmission. Based on the control information embedded in unused field in the HE preambles, the SR initiator adaptively controls transmission power and modulation and coding scheme (MCS) to protect both ongoing and SR transmissions. Through extensive ns-3 simulations, we show that *OSR* significantly improves the throughput compared with the legacy 802.11n and baseline OBSS PD.

We conclude the dissertation in Chapter 4.

Chapter 2

BeaconRider: Opportunistic Sharing of Beacon Air-Time in Densely Deployed WLANs

2.1 Introduction

The proliferation of mobile devices has resulted in explosive traffic growth which is expected to reach 49 exabytes per month globally [29]. As cellular spectra and network resources become taxed, wireless local area networks (WLANs) have been utilized to offload mobile traffic [30, 31]. It is reported that 60% of global mobile data traffic has been offloaded to WLANs in 2016 [29].

The upsurge in IEEE 802.11 WLAN traffic has led to dense deployment of access points (APs) in urban areas including office buildings, residential housing, shopping malls, public spaces, among many others. As density of APs increases, the number of APs that a wireless station (STA) can access increases, leading to interference between nearby APs. As a consequence, interference induced by management frames (e.g., beacon frame) also increases, which can significantly degrade system performance.

In this chapter, we focus on the problem of air-time depletion due to beacon transmissions which are essential for the operation of a basic service set (BSS)[1]. Beacon

[1] A BSS consists of an AP and multiple associated STAs.

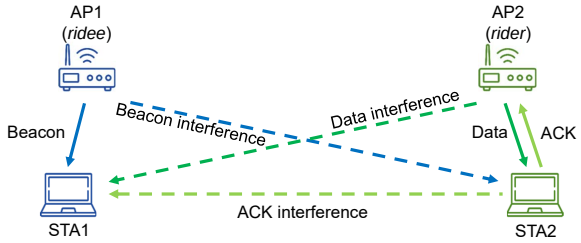

Figure 2.1: Example of simultaneous transmission of beacon and data frames.

frames are transmitted at the lowest basic transmission rate to ensure reliable delivery to STAs associated with a BSS. This implies that each beacon frame occupies considerable air-time despite its short length. If a STA is within the range of multiple APs, it will be exposed to a large number of beacon frames which can take up a significant portion of its air-time. Our experiments indicate that up to 43.9% can be taken up by beacon frames, which leads to significant reduction of air-time for data transmissions.

To address the air-time depletion problem, we introduce a new approach of air-time sharing that allows simultaneous data transmission during the air-time of beacon transmission of neighboring APs. Fig. 2.1 depicts an example of two pairs of AP and STA, where one of the APs (AP2) initiates data transmission while the other (AP1) is transmitting a beacon frame. The dotted lines indicate potential interference across the two BSSs that cause frame decoding failure at the receiving STA of the other BSS. However, the interference does not always lead to the decoding failure thanks to the capture effect. Since a beacon frame is transmitted at the lowest transmission rate, the beacon decoding at STA1 may succeed if data/ACK transmission interference from AP2/STA2 is not sufficiently strong. In addition, whether the capture effect leads to successful decoding of the data frame at STA2 will depend on its transmission rate and strength of beacon interference.

Our goal is to exploit the signal diversity of wireless communication by opportunistically engaging in simultaneous data transmission in the presence of beacon transmission. To this end, we develop a distributed protocol that explicitly exploits the capture effect based on real-world measurement characteristics and coordinates

air-time sharing in an efficient and reliable manner. The protocol selects two appropriate APs such that the beacon frame is sufficiently protected from the interference of the data-ACK transmissions, and at the same time, data-ACK transmissions are likely to be successful under beacon interference.

Our main contributions are as follows.

- Based on beacon frame traces in real-world environments, we analyze the characteristics of beacon frames and their impact on system performance.
- We develop an opportunistic air-time sharing protocol, *BeaconRider*, that allows simultaneous data transmission during the beacon period of neighboring APs. The proposed method provides distributed coordination between APs without incurring additional control message exchange.
- We implement the protocol on an off-the-shelf IEEE 802.11n dongle using the *ath9k-htc* open-source firmware [32] which operates as an AP. The modified APs coexist with legacy APs and do not require any changes at STAs. These properties facilitate partial deployment of *BeaconRider*.
- Through experiments with a prototype implementation and extensive simulation using ns-3 [33] under a variety of network environments, we demonstrate that *BeaconRider* significantly improves throughput performance.

To the best of our knowledge, this is the first work that shares beacon air-time for data transmission by exploiting the capture effect.

The rest of this chapter is organized as follows. In Section 2.2, we describe motivation of our work. Section 3.3 presents a detailed design of *BeaconRider*. In Section 2.4, based on measurements and analysis, we gauge reliability of beacon frames under riding data interference. We evaluate the performance of *BeaconRider* via experiment and simulation in Section 3.4. Finally, we summarize this chapter in Section 3.5.

2.2 Beacon congestion problem

In IEEE 802.11 WLANs, APs periodically transmit beacon frames to announce their network information. In this chpter, we consider an infrastructure BSS where only APs transmit beacon frames. Beacon frames are typically transmitted at an interval of 102.4 ms [30], at the lowest basic (mandatory) transmission rate for reliability, e.g., at 1 Mbps in 2.4 GHz band and at 6 Mbps in 5 GHz band. As a consequence, beacon frames often take up more air-time than data frames despite their short length. As the density of BSSs increases, a large portion of air-time is consumed by beacon frames, which is referred to as the *beacon congestion problem*.

For advanced network services, vendors may tag additional information onto beacon frames as optional fields, which aggravates the beacon congestion problem. The problem is more severe in the 2.4 GHz band due to lower beacon transmission rate and smaller number of available channels. Moreover, a large portion of WLAN devices still support 2.4 GHz band only, and dual-band devices that support both 2.4 GHz and 5 GHz bands may prefer 2.4 GHz band due to propagation advantages of the 2.4 GHz band [34–36]. In this chapter, we focus on mitigating the beacon congestion problem in the 2.4 GHz band since it is more pronounced.

To quantify the impact of beacon congestion, we used *Wireshark* [37] to collect beacon frame traces (total 3,218 distinct APs) in several real-world WLAN networks across campus buildings, commercial WLAN hotspots at shopping malls, subway stations, coffee shops, and movie theaters. The trace results are shown in Fig. 2.2. The distribution of beacon air-time duration in Fig. 2.2(a) shows the impact of a single beacon frame on air-time depletion. The minimum, maximum, and average of the beacon air-time duration are summarized in Table 2.1. Considering the default beacon interval of 102.4 ms, average duration of a single beacon frame accounts for about 2.1% of total air-time. When coverage spans multiple APs, beacon congestion deteriorates depending on the number of APs observed by a STA.

The distribution of the number of observed APs in a single channel is shown in

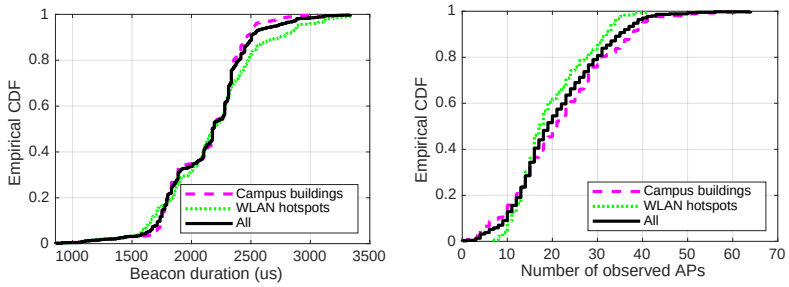

(a) Distribution of beacon air-time duration

(b) Distribution of the number of observed APs per channel

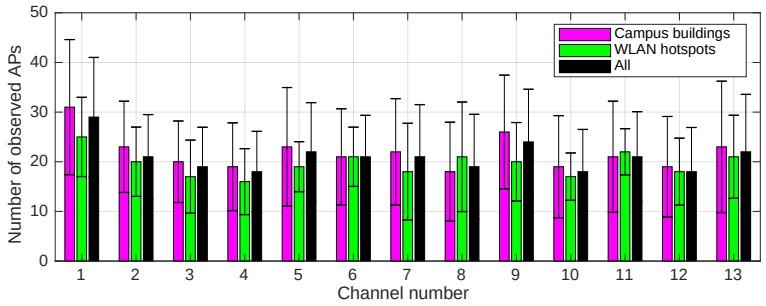

(c) The number of observed APs at each channel in 2.4 GHz band

Figure 2.2: Statistics of beacon frames in practical WLANs. Total 3,218 beacon frames are collected from 20 campus buildings and 14 commercial WLAN hotspots.

Fig. 2.2(b), and the values are summarized in Table 2.1. A single STA observes 21 beacon frames on average in a typical beacon interval of 102.4 ms, where the average duration of a single beacon frame is 2,140 μs. This results in 43.9% air-time consumption from beacon sensing, which significantly limits air-time available for data transmissions.

Fig. 2.2(c) shows the number of observed APs at each channel in the 2.4 GHz band. Although the number of observed APs in non-overlapped channels (i.e., channels 1, 5, 9, and 13) is larger than that in other channels, a significant number of APs are also observed in other channels as well. This shows the beacon congestion problem is not limited to the non-overlapped channels. In this sense, we observed that beacon transmission in one channel can be detected in partially overlapped channels [38]. This further exacerbates beacon congestion.

Table 2.1: Summary of beacon frame statistics

Parameters		Campus buildings	WLAN hotspots	All
Air-time duration of one beacon frame (μs)	Min.	856	864	856
	Max.	3,064	3,336	3,336
	Avg.	2,120	2,182	2,140
The number of observed APs per channel	Min.	0	7	0
	Max.	64	41	64
	Avg.	22	20	21

2.3 Design of *BeaconRider*

In this section, we propose *BeaconRider*, an air-time sharing scheme that allows simultaneous data transmission during the air-time of beacon transmission, by explicitly exploiting the capture effect. We first provide the overview of *BeaconRider*, and explain its operation in detail.

2.3.1 Overview of *BeaconRider*

We implement *BeaconRider* at the AP side, and denote the AP with our scheme by *BeaconRider* AP, or simply BAP. When we use the term AP, it is either a BAP or a legacy AP. In Fig. 2.1, we denote the left AP transmitting the beacon frame by *ridee* and the right AP transmitting data by *rider*. In our design, we let the ridee select the rider AP to transmit data frames while transmitting beacon frames.

Successful riding and beacon reception need coordination between BAPs. To avoid additional control message exchange for the coordination, we redefine three fields of the IEEE 802.11 beacon frame: *power management (PM)*, *more data (MD)* subfields, and *source address (SA)* field, marked in Fig. 2.3. Note that the PM and MD subfields

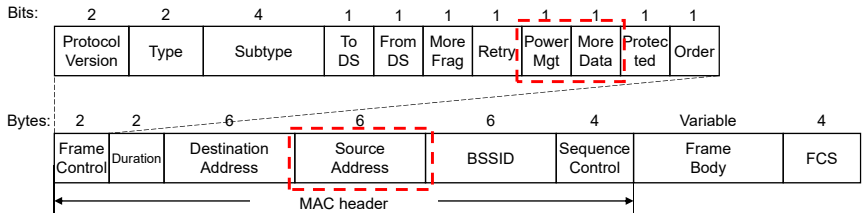

Figure 2.3: Frame structure of the IEEE 802.11 beacon frame. Marked fields are of active use under *BeaconRider* for the coordination between APs.

are reserved (i.e., not used), and the SA field is a duplicate of the BSSID field[2]. We use the PM and MD subfields as the BAP indicator and the buffer status indicator, respectively. The BAP sets the PM bit for each beacon frame, and sets the MD bit when it has data traffic to transmit. The SA field plays a key role in coordination. The ridee uses this field to grant riding to the rider. We explain the overall operation through the following three actions.

1. **Listening:** A BAP listens to beacon frames from neighboring (B)APs, and collects information needed to determine whether it becomes a ridee or not. Using the information, it selects one of neighboring BAPs as its corresponding (target) rider. The selection may change over time according to the channel state.

2. **Informing rider selection:** When transmitting beacon frames, each BAP (as a ridee) informs its neighboring APs of the latest decision on rider selection through using the SA field of the beacon frame.

3. **Riding:** While receiving a beacon frame, the BAP quickly checks the SA field in the beacon frame. If the receiving BAP is indicated as the target rider of

[2]According to the 802.11 standard [30], the PM subfield is used to indicate the PSM status of a STA, and the MD subfield is valid only in individually addressed data frame or management frame. For the SA field, the implementation cases that we tested, e.g., *ath9k* and *android* [39], use only the BSSID field of the received beacon frame to identify the beacon transmitter and does not refer to the SA field. There may be some legacy implementations that access the SA field for this purpose, which may need further investigation.

the beacon frame, it immediately stops receiving the beacon frame and starts transmitting a data frame, thus attempting to ride the beacon frame.

2.3.2 Operation of Ridee

The important task of the ridee is to select the right riding BAP, enabled to share its beacon air-time. The transmissions of beacon and riding data-ACK frames should not interfere with each other. Moreover, AP coordination should proceed without a central entity or additional control message exchange, conforming to the distributed nature of the WLAN protocol and backward compatibility.

In our scheme, the BAP continues listening to beacon frames from its neighboring APs, and collecting the information of beacon length, received signal strength (RSS), BSSID, buffer status (i.e., MD bit), and BAP indication (i.e., PM bit). If the beacon transmitter is a BAP, it computes average RSS through exponential weighted moving average (EWMA). By default, we set the weight factor of EWMA to 0.125.

At every beacon transmission, the ridee selects the BAP with the lowest average RSS as the rider, among the list of neighboring BAPs with non-empty buffer. The ridee informs neighboring BAPs of the decision on rider selection by setting the SA field of the beacon frame to the MAC address of the target rider.

2.3.3 Operation of Rider

Upon receiving a beacon frame, the BAP begins to decode its SA field. If the MAC address in the SA field matches with its own MAC address, the BAP operates as the rider of the beacon frame, i.e., immediately stops receiving the beacon frame and starts to transmit a data frame.

Note that the beacon reception is protected from the interference of data transmission through the sender-first capture: the beacon frame transmitted at the lowest MCS level (i.e., 1 Mbps) always precedes a riding data frame. In this scenario, the capture effect is easily triggered since a low SIR threshold (-10 dB as shown in Section 2.4) is

required and the RSS from the selected rider is the lowest among neighboring BAPs.

On the other hand, the beacon reception may not be protected from the interference of ACK transmission if the riding data receiver is close to the beacon receiver. Also, it is possible that the riding data transmission fails due to the beacon interference. To address these problems, we carefully choose the data frame length, the MCS level, and the final decision on a riding attempt at the rider.

Selection of the data frame length for riding

Unlike the interference from riding data transmission, the interference due to ACK transmission paired with riding data transmission can be significant and disrupt the beacon reception. The interference level highly depends on the location of the receiver. To avoid such uncertainties, *BeaconRider* controls the length of the riding data frame by aggregating several subframes such that the transmission of aggregated riding data frame lasts longer than the beacon transmission, which ensures no transmission overlap between the beacon frame and the block ACK (BlockACK) frame paired with the riding data frame[3].

An example is shown in Fig. 2.4. Let t_{detect} and t_{delay} denote the times for the rider to detect the beacon frame and to prepare for riding, respectively, and t_{beacon} be the beacon duration[4]. For given MCS level x for riding transmission, we easily obtain the smallest number of subframes such that the riding data transmission is not completed earlier than the beacon transmission (i.e., $t_{\mathrm{detect}} + t_{\mathrm{delay}} + t^{x}_{\mathrm{riding}} \geq t_{\mathrm{beacon}}$), and set it as the length of the riding data frame.

[3]Recent WLAN standards (IEEE 802.11n/ac) [30, 31] support *frame aggregation*, under which multiple MAC protocol data unit (MPDU) frames are aggregated into a single aggregate MPDU (A-MPDU) frame, and the receiver positively/negatively acknowledges all individual subframes (i.e., MPDUs) by using a BlockACK, which allows selective retransmission of subframes.

[4]t_{detect} and t_{delay} can be measured online by using a local time function in the firmware in our implementation, which are around 400 μs and 100 μs, respectively. We expect that these delays decrease further in recent devices. Finally, t_{beacon} can be easily obtained from the beacon length.

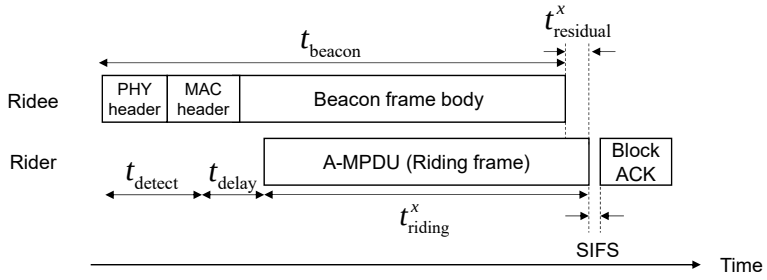

Figure 2.4: Timeline example of riding data-ACK transmissions.

Selection of the MCS level for riding

Another important decision that the rider BAP should make is about the MCS level for data frame transmission. From the viewpoint of the receiver of the riding data frame, on-going beacon transmission appears as interference. As a result, the rider may need to lower its MCS level than usual.

To find the right MCS level, we define a utility function for each MCS level using subframe error rate (SFER). To elaborate, suppose that the MCS level for a (non-riding) data transmission is m. The level is usually determined by a built-in rate adaptation algorithm according to the channel condition of the receiver, given by signal-to-noise-ratio (SNR) or frame error rate (FER). When MCS level x is used for riding when m is given, after a riding attempt, the rider BAP counts the number of non-acknowledged[5] subframes in the corresponding BlockACK and computes average SFER $\tilde{e}^i_{m,x}$ for ridee i through EWMA with weight factor of 0.125. The utility $U^i_{m,x}$ of MCS x given m is updated as

$$U^i_{m,x} = r_x \cdot \left(1 - \tilde{e}^i_{m,x}\right) \cdot t^x_{\text{riding}} - r_m \cdot t^x_{\text{residual}}, \tag{2.1}$$

where r_x denotes the transmission rate under MCS x, and t^x_{riding} and t^x_{residual} denote the riding duration and the residual time under MCS x, respectively, as shown in Fig. 2.4. Roughly, the utility represents the effective gain of riding transmission under MCS x over a (non-riding) data frame transmission under MCS m. The first term

[5]If the BlockACK does not arrive, we consider that all the subframes are not acknowledged.

can be considered as a gain of air-time sharing and the second term as a loss in the case of reception failure. In the next riding, the rider chooses the MCS level x^* with the highest utility, i.e., $x^* = \arg\max_x U^i_{m,x}$. We break a tie arbitrarily.

Under the disturbance in signal strength (e.g., fading), it may occur that our MCS selection remains at low levels since SFER is only updated after a riding attempt. To avoid this, we conditionally explore the next higher MCS level if the same MCS level has been used multiple times in a row. Let p^i_{win} (> 0) and p^i_{cnt} (≥ 0) as the window size of exploration back-off and the remaining number of riding trials before the rider explores the next higher MCS level for ridee i, respectively. Both are set to 1 initially. When the BAP tries a riding transmission with the same MCS (m, x) as the previous riding, it decreases p^i_{cnt} by one. Otherwise, it sets $p^i_{\text{cnt}} = p^i_{\text{win}}$. If p^i_{cnt} reaches 0, the BAP explores the next higher MCS level at the next riding. If the exploration is successful, the BAP halves p^i_{win} and sets $p^i_{\text{cnt}} = p^i_{\text{win}}$. Otherwise, it doubles p^i_{win} and sets $p^i_{\text{cnt}} = p^i_{\text{win}}$.

Adaptive riding (AR)

Despite the utility-based selection of the MCS level, success of a riding transmission highly depends on the interference from the ridee's beacon transmission. If the riding transmission fails, we lose t^x_{residual} amount of air-time. Hence, in case that the interference from the beacon transmission is significant, it may be better not to attempt riding. To this end, we develop a simple adaptive riding-attempt (AR) algorithm. We define two parameters g^i_{win} (> 0) and g^i_{cnt} (≥ 0) as the window size of riding back-off and the remaining number of riding back-offs before the rider resumes riding for ridee i, respectively. We initially set g^i_{win} and g^i_{cnt} as 1 and 0, respectively. When the rider has $U^i_{m,x} < 0$ for all x due to high SFER, it sets $g^i_{\text{cnt}} = g^i_{\text{win}}$ and stops riding. Upon receiving a beacon frame from ridee i, the rider decreases g^i_{cnt} by one. When g^i_{cnt} reaches 0, the rider resumes riding with the lowest MCS level. If the riding attempt fails again, the rider doubles g^i_{win}, sets $g^i_{\text{cnt}} = g^i_{\text{win}}$, and repeats the g^i_{cnt}-decreasing procedure. On any riding attempt success, the rider halves g^i_{win} (down to 1) and sets $g^i_{\text{cnt}} = 0$.

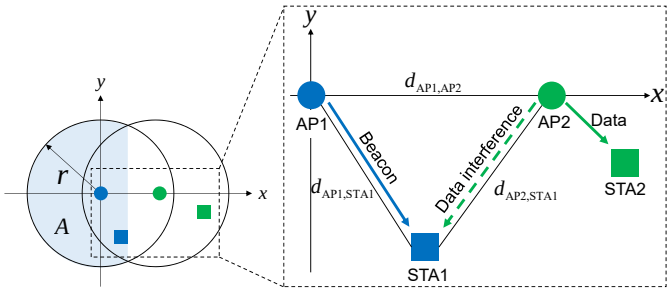

Figure 2.5: Example of two BSSs. Each STA is associated with the closest AP in terms of received signal strength (RSS), and the shaded area (A) is the coverage of AP1.

2.4 Reliability of Beacon Transmission

An interesting feature of *BeaconRider* is that riding permission is granted by the ridee. Specifically, if the ridee suffers difficulty in beacon frame delivery, it easily stops allowing riding by filling the SA field with its own MAC address. Nevertheless, it is important to estimate the impact of riding on the beacon reception. In this section, we investigate reliability of the beacon reception under riding scenarios. We first model the beacon frame error rate (BFER) according to the location of the STA. Then, using the measured beacon reception ratio (BRR), we numerically calculate the expected BFER within the coverage of an AP. Lastly, we propose a simple algorithm to detect a beacon loss at STAs to eliminate corner cases.

2.4.1 Beacon Frame Error Rate (BFER)

We consider two BSSs as shown in Fig. 2.5, where AP1 (ridee) transmits a beacon frame to STA1, and AP2 (rider) transmits a riding data frame to STA2. We denote $d_{i,j}$ the distance between node i and node j. Without loss of generality, AP1 and AP2 are located at the origin (0,0) and ($d_{\mathrm{AP1,AP2}}$, 0), respectively. Suppose that STAs are randomly located in the space, and associated with the closest AP in terms of RSS. A STA communicates with an AP if they are within distance r.

We model the wireless channel gain between a STA and an AP according to their distance. Let $L_{i,j}$ denote the channel gain from node i to node j, where a node is either an AP or a STA. The channel gain is given as

$$L_{i,j} = \Gamma_{i,j} \cdot L_0 \cdot d_{i,j}^{-\alpha}, \tag{2.2}$$

where α and L_0 denote the pathloss exponent and a fixed loss, respectively, and $\Gamma_{i,j} \sim \mathrm{Exp}(1)$ is a Rayleigh fast fading component with a unit average power. Assuming mutually independent $\Gamma_{i,j}$ and the channel reciprocity for any pair of nodes, the signal power from AP1 to STA1 can be written as $S_{\mathrm{AP1}\to\mathrm{STA1}} = P_{\mathrm{AP1}} \cdot G_{\mathrm{AP1}} \cdot G_{\mathrm{STA1}} \cdot L_{\mathrm{AP1,STA1}}$, where P_i and G_i denote the transmission power and the antenna gain at node i, respectively. The data interference from AP2 to STA1 can be similarly obtained as $I_{\mathrm{AP2}\to\mathrm{STA1}} = P_{\mathrm{AP2}} \cdot G_{\mathrm{AP2}} \cdot G_{\mathrm{STA1}} \cdot L_{\mathrm{AP2,STA1}}$.

Assuming the noise is negligible compared to the interference and $P_{\mathrm{AP1}} \cdot G_{\mathrm{AP1}} = P_{\mathrm{AP2}} \cdot G_{\mathrm{AP2}}$, the SIR at STA1 can be written as

$$\mathrm{SIR}_{\mathrm{STA1}} = \frac{S_{\mathrm{AP1}\to\mathrm{STA1}}}{I_{\mathrm{AP2}\to\mathrm{STA1}}} = \frac{\Gamma_{\mathrm{AP1,STA1}}}{\Gamma_{\mathrm{AP2,STA1}}} \left(\frac{d_{\mathrm{AP1,STA1}}}{d_{\mathrm{AP2,STA1}}}\right)^{-\alpha}. \tag{2.3}$$

Note that the probability density function (PDF) of a random variable Z, defined as the ratio of two independent and identically distributed (i.i.d.) exponential random variables, is known as $f_Z(z) = \Pr(Z = z) = \frac{1}{(z+1)^2}$ [40]. Since $\Gamma_{\mathrm{AP1,STA1}}$ and $\Gamma_{\mathrm{AP2,STA1}}$ are i.i.d. exponential random variables with a unit variance, we obtain the PDF of the SIR which depends on $\gamma = \left(\frac{d_{\mathrm{AP1,STA1}}}{d_{\mathrm{AP2,STA1}}}\right)^{-\alpha}$ as

$$f_\gamma(\rho) = \frac{1}{\gamma} \cdot \frac{1}{\left(\frac{\rho}{\gamma} + 1\right)^2}, \tag{2.4}$$

where ρ represents the SIR value. Given the STA's location (x, y), we obtain the expected BFER as

$$\overline{\mathrm{BFER}}(x, y) = \int_0^\infty \mathrm{BFER}(\rho) \cdot f_{\gamma_{xy}}(\rho) d\rho, \tag{2.5}$$

where $\mathrm{BFER}(\rho)$ is the BFER for given ρ.

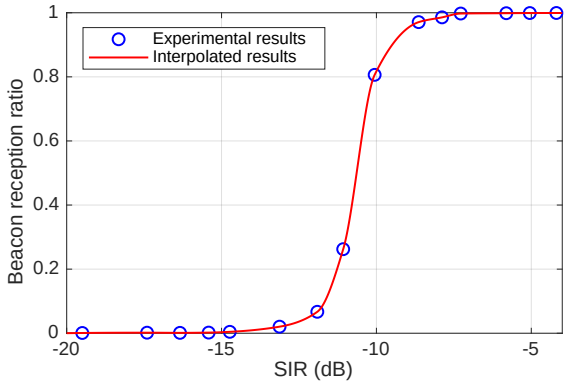

Figure 2.6: Measurements on the beacon reception ratio (BRR) according to the SIR value. Beacon frames of 280 bytes are transmitted at rate 1 Mbps. We averaged 5 measurements, and each iteration lasts for 3 minutes. The red line is obtained by interpolating experimental results.

2.4.2 Measurement-based Calculation of Beacon Reception Ratio (BRR)

There have been several studies to model the FER, but they did not take the sender-first capture into consideration, thus leading to an overestimation of BFER in our riding scenario [41, 42]. To design a precise model of $\mathrm{BFER}\,(\rho)$, we conduct experiments in our testbed as follows.

We deploy a couple of AP-STA pairs as shown in Fig. 2.5. We set the distance between AP1 and AP2 as 5 m. While AP1 transmits beacon frames periodically, AP2 generates saturated UDP downlink traffic toward STA2 for 3 minutes. Whenever AP2 detects a beacon frame of AP1, it immediately transmits a riding data frame. In the experiments, we count the number of successfully received beacon frames at STA1 and the number of total transmitted beacon frames from AP1, and take their ratio to obtain the BRR. We repeat the measurements under different SIR configurations at STA1 by changing the transmission power of AP1 from 0 to 15 dBm, while fixing that of AP2 to 20 dBm.

Fig. 2.6 shows the BRR of STA1 according to the SIR value. The BRR sharply

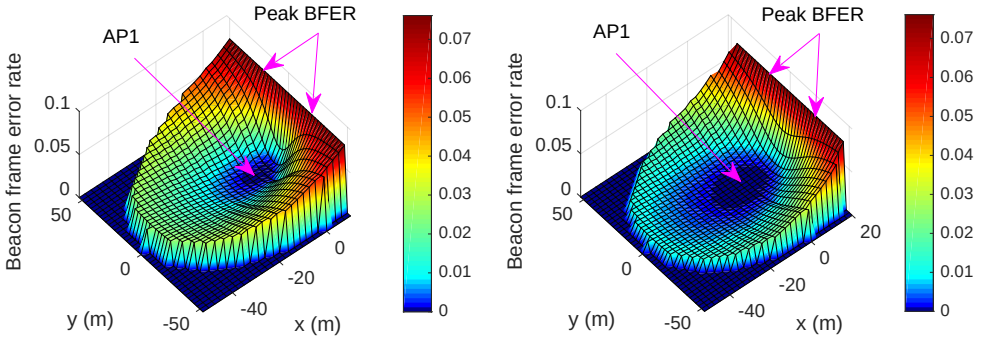

(a) $r = 50$, $d_{\mathrm{AP1,AP2}} = 20$

(b) $r = 50$, $d_{\mathrm{AP1,AP2}} = 40$

Figure 2.7: Expected beacon frame error rate (BFER) according to the STA's location (x, y). The peak BFER (7.6%) is observed at line $x = d_{\mathrm{AP1,AP2}}/2$.

rises from zero to one around the SIR of -11 dB. This is because, below the threshold, the sender-last capture occurs, and STA1 receives a data frame from AP2, not a beacon frame from AP1. From the results, we observe that the required SIR threshold to capture the beacon frame is very small (around -10 dB), which implies that the beacon frame can be easily captured when the STA associates with the AP of the strongest signal strength. From $\mathrm{BFER}(\rho) = 1 - \mathrm{BRR}(\rho)$, we use the measurement results to compute $\overline{\mathrm{BFER}}(x, y)$ in (2.5).

2.4.3 Numerical Results

We numerically obtain $\overline{\mathrm{BFER}}(x, y)$ for different values r and $d_{\mathrm{AP1,AP2}}$, which is shown in Fig. 2.7. As expected, $\overline{\mathrm{BFER}}(x, y)$ decreases as STA1 moves toward AP1 (or away from AP2). We can observe the peak BFER (7.6%) at line $x = d_{\mathrm{AP1,AP2}}/2$, which is the same regardless of $(r, d_{\mathrm{AP1,AP2}})$. By integrating $\overline{\mathrm{BFER}}(x, y)$ over the coverage of AP1, i.e., the shaded area (A) in Fig. 2.5, we obtain the average BFER of a randomly deployed STA as

$$\overline{\mathrm{BFER}}_{\mathrm{AP1}} = \int_A \overline{\mathrm{BFER}}(x, y) dx dy. \tag{2.6}$$

In our results, we observe that $\overline{\mathrm{BFER}}_{\mathrm{AP1}}$ decreases from 3.0% to 1.7% as the ratio $\frac{r}{d_{\mathrm{AP1,AP2}}}$ decreases. This is due to reduced interference from riding data transmission.

In summary, our measurements show that beacon frames are rarely lost under the interference from riding data transmission due to the sender-first capture, and well protected by selecting the rider with the least RSS.

2.4.4 Beacon Loss Detection

Although beacon frames are well protected under our rider selection and riding data frame length selection algorithms, it is still important to detect a beacon loss to eliminate corner cases. Unfortunately, there is no explicit way at the AP side to detect a beacon loss at STAs since the beacon does not require any response (i.e., ACK frame). Instead, at the STA side, if an STA misses k beacons in a row ($k = 10$ in *ath9k* driver and ns-3 simulator by default), it considers the connection is lost and initializes the reassociation procedure by sending a probe request frame. Hence, the AP can use the probe request frame from an STA to detect a beacon loss.

2.5 Performance Evaluation

In this section, we evaluate the performance of *BeaconRider* through prototype implementations and experiments. We present the results of extensive simulations with ns-3 for its performance in a wide range of network environments.

2.5.1 Prototype Implementation

We have implemented the prototype of *BeaconRider* over an off-the-shelf IEEE 802.11n dongle (TP-Link WN722N v1) with Qualcomm Atheros AR9271 and the open-source firmware of *ath9k-htc*. The source code is available at [43]. The block diagram of *BeaconRider* is illustrated in Fig. 2.8.

On receiving a beacon frame, the *beacon information management* block collects

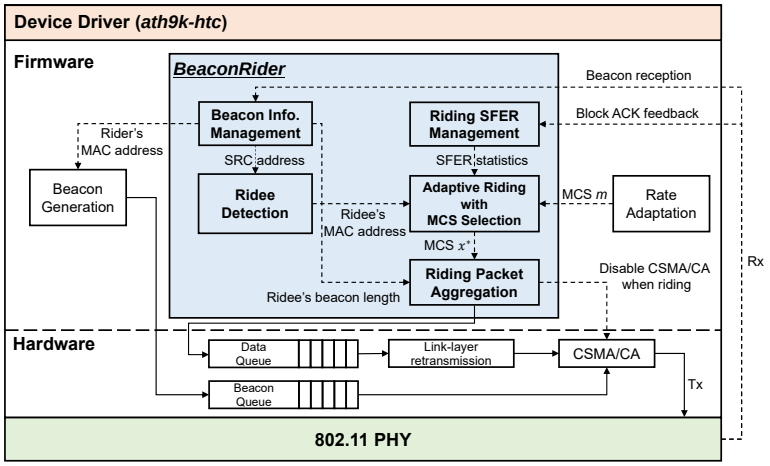

Figure 2.8: Block diagram of *BeaconRider*.

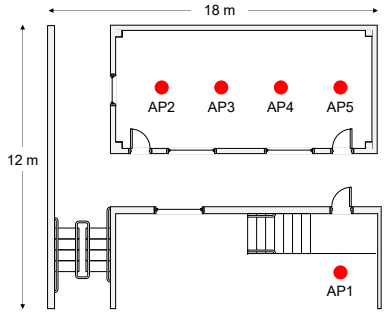

Figure 2.9: Floor plan.

necessary information from the beacon frame's MAC header. To perform real-time monitoring of the receive buffer, we use direct memory access (DMA) function as in [44]. Using the information, the *ridee detection* block triggers riding transmission, and then the *adaptive riding with MCS selection* block makes a riding decision on an appropriate MCS level, according to SFER statistics. Once the decision is made, a riding data frame is prepared in the *riding packet aggregation* block, put in the data queue, and immediately transmitted by disabling CSMA/CA.

Experimental settings:

We first conduct basic experiments in a controlled office environment as shown

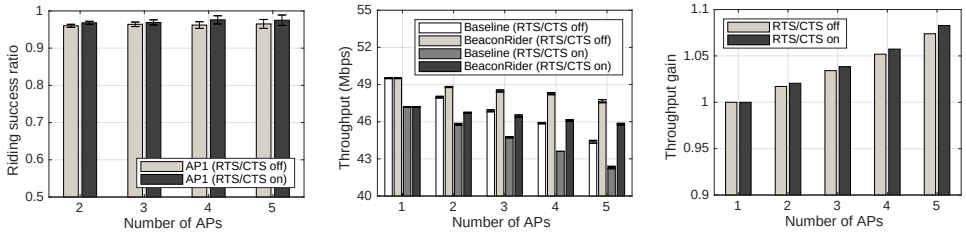

(a) Riding success ratio (RSR) (b) Throughput (c) Throughput gain

Figure 2.10: Riding success ratio (RSR), throughput, and throughput gain for a single-source scenario.

in Fig. 2.9. Each point represents an AP, and one STA per AP is placed within 1 m distance from its associated AP[6]. For each AP, we use *hostapd* 2.6 [45] on ubuntu 14.04 over a laptop (Samsung NT531U4E) with an IEEE 802.11n dongle. As a STA, we use a desktop PC with Qualcomm Atheros AR9380 Network Interface Card (NIC). Otherwise specified, we use channel 10 centered at 2.457 GHz (after checking no external interference), and set the beacon frame length to 280 bytes. When an AP has data traffic for its associated STA, we generate UDP traffic using *Iperf* 2.0.5 and saturate the link. For each experiment, the results are averaged over 5 runs, where each run lasts for 120 s.

Results: We first consider the scenario when only one of APs (i.e., AP1) has data traffic to send, and the other APs (AP2 to AP5) do not have data traffic and can be either active (on) or inactive (off). Thus, AP1 is the only rider among all active APs.

We evaluate the riding performance of AP1, through the ratio of the number of successful riding transmissions to the number of total riding trials, denoted as riding success ratio (RSR). Fig. 2.10(a) shows the results, where AP1 achieves high RSR for all the cases. This implies that riding data-ACK transmissions are well protected under the beacon interference. Also, we can observe that the impact of RTS/CTS on the RSR is negligible.

[6]We consider BSSs where only one STA is associated with an AP for experimental simplicity. Nevertheless, our scheme can simply support multiple STAs by managing SFER statistics for each ridee and receiver STA pair independently.

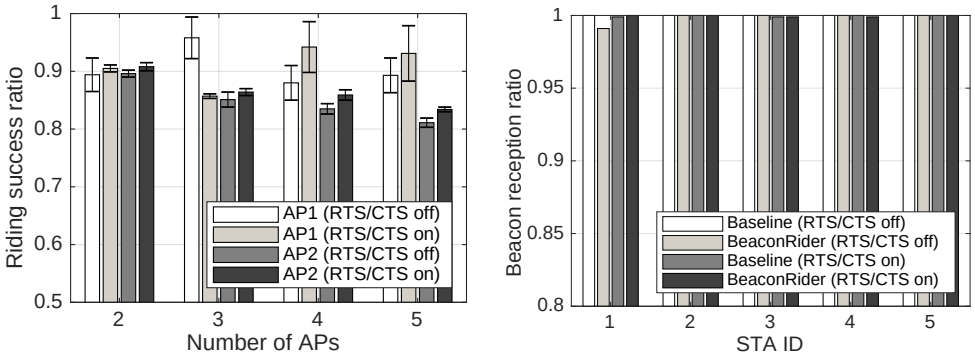

(a) Riding success ratio (RSR)

(b) Beacon reception ratio (BRR)

Figure 2.11: Riding success ratio (RSR) and beacon reception ratio (BRR) for a multi-source scenario.

Fig. 2.10(b) shows throughput performance in the same scenario. For performance comparison, we use IEEE 802.11n as the *baseline*. It shows that, as expected, the total throughput linearly decreases as the number of active APs increases for both the baseline and *BeaconRider*. However, *BeaconRider* experiences much less performance degradation since it compensates a significant amount of air-time loss through air-time sharing. Fig. 2.10(c) illustrates the throughput gains of *BeaconRider* against the baseline according to the number of active APs, which clearly shows a linear relationship between the performance gain and the number of active APs. An interesting result is that when RTS/CTS is on, throughput performance decreases further for both the baseline and *BeaconRider*. This is due to additional overhead (or air-time consumption) incurred by RTS/CTS exchange for each data transmission. On the other hand, throughput gains of *BeaconRider* are enhanced under RTS/CTS as shown in Fig. 2.10(c) since *BeaconRider* initializes riding transmissions without incurring any overhead.

Next, we consider a multi-source scenario where all active APs have data traffic to send. In this case, AP1 and AP2 become the rider of AP2-5 and AP1, respectively. Fig. 2.11(a) shows the RSR values, which are lower than those in the single-source scenario.

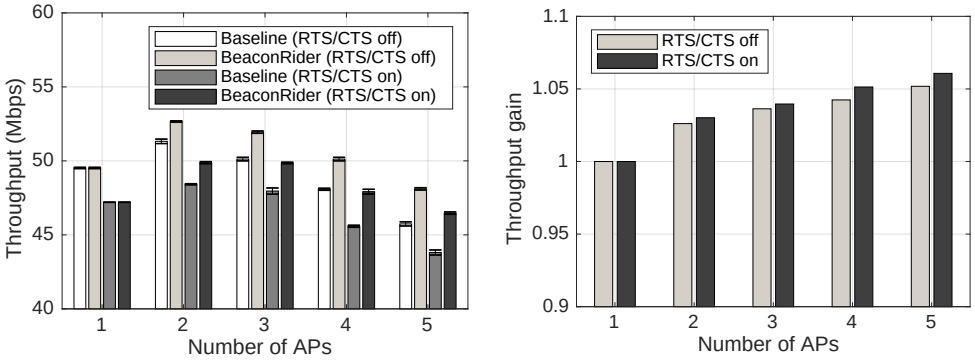

(a) Throughput

(b) Throughput gain

Figure 2.12: Throughput and throughput gain for a multi-source scenario.

We observed that when the ridee AP has data traffic, it occasionally tries a data transmission during the residual time t^x_{residual} of riding transmission when it fails to detect the ongoing riding data-ACK frame transmissions due to the high threshold value for energy detection (i.e., -62 dBm). In that case, the rider often fails to receive BlockACK correctly even under high SIR conditions. We conjecture this is due to the limited capability of our dongle (TP-LINK WN722N v1), which results in slightly degraded performance of *BeaconRider*.

Fig. 2.11(b) shows the BRR of each individual STA when there are 5 APs. We can observe all the BRR values are close to 1, and thus, the beacon reception is well protected from the interference of riding data transmissions. For BRR, similar results are obtained for the case of 2-4 APs, which are omitted. Fig. 2.12(a) and Fig. 2.12(b) show the total throughput under the baseline and *BeaconRider*, and the gain of *BeaconRider* against the baseline. We observe a multiplexing gain when two APs generate traffic. Afterward, the performance linearly degrades due to the beacon congestion under the baseline and *BeaconRider*, but the degradation under *BeaconRider* is much milder. As before, the performance gain tends to linearly increase with the number of APs, and gets better under RTS/CTS.

We now investigate the impact of MCS selection and adaptive riding (AR) on RSR and throughput in *BeaconRider*. Choosing the optimal MCS level for riding transmis-

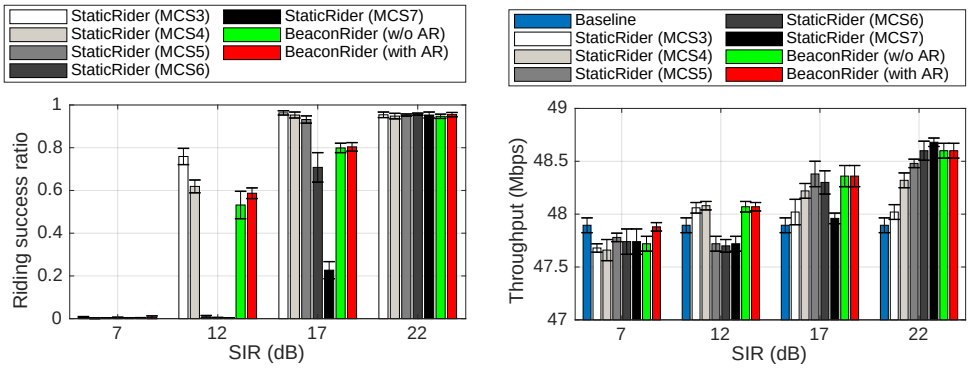

(a) Riding success ratio (RSR)

(b) Throughput

Figure 2.13: Impact of MCS selection and adaptive riding (AR) on RSR and throughput.

sion is crucial to achieve high riding performance. To this end, we build a network of two AP-STA pairs as shown in Fig. 2.5: the distance between AP1 and AP2 is set to 5 m, and STA2 is located between AP1 and AP2. AP1 and AP2 are the ridee and rider, respectively, and AP2 has saturated data traffic destined to STA2. We configure the SIR at STA2 by controlling the AP's transmission power: the transmission power of AP1 is set to a value in $[0, 15]$ dBm, and that of AP2 is fixed to 20 dBm, which corresponds to the SIR of $[7, 22]$ dB at STA2. We evaluate the performance of the baseline 802.11n, *BeaconRider* with a fixed MCS level for riding and without AR (denoted as *StaticRider*), and *BeaconRider* with our MCS selection and without AR, and *BeaconRider*.

Fig. 2.13(a) and Fig. 2.13(b) show their performance in terms of RSR and throughput according to different SIR configurations. From Fig. 2.13(a), we observe that riding transmissions with high MCS levels often fail when the SIR is low (e.g., 12 dB). On the other hand, riding transmissions with low MCS levels result in low throughput gain when the SIR is high (e.g., 22 dB) as shown in Fig. 2.13(b). In contrast, *BeaconRider* with or without AR selects a right MCS level and thus achieves good performance for most SIR configurations.

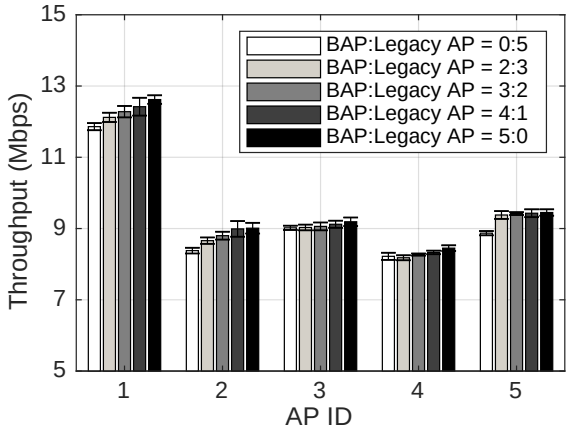

Figure 2.14: Throughput of each AP under the coexistence of BAPs and legacy APs.

An interesting point is that, when the SIR is 12 dB, *StaticRider*s with MCS 5-7 achieve even worse performance compared to the baseline. This is because their riding transmissions require higher overhead (i.e. longer residual time) due to lower transmission rate, and thus consume more air-time without contributing to throughput improvement since most of them fail as shown in Fig. 2.13(a). It shows that the MCS selection indeed plays a critical role to improve riding performance. In the case when the SIR is very low (e.g., 7 dB), riding transmissions often fail since their signal strength is lower than the capture threshold. In this case, *BeaconRider* with AR outperforms that without AR by refraining from riding, and achieves the performance comparable to the baseline.

In practice, there may be external interference in the ISM band, which comes from electronic devices such as microwaves, and other communication technologies like Bluetooth and Zigbee. A concern is that they may interfere with the operation of *BeaconRider*, leading to a worse performance compared to the baseline. However, *BeaconRider* performs well at least as the baseline since it operates in a conservative manner using the MCS selection and AR algorithms.

We also consider the coexistence scenario of BAPs and legacy APs. We deploy 5 APs and 5 STAs, and change the number of BAPs out of 5 APs. We measure the

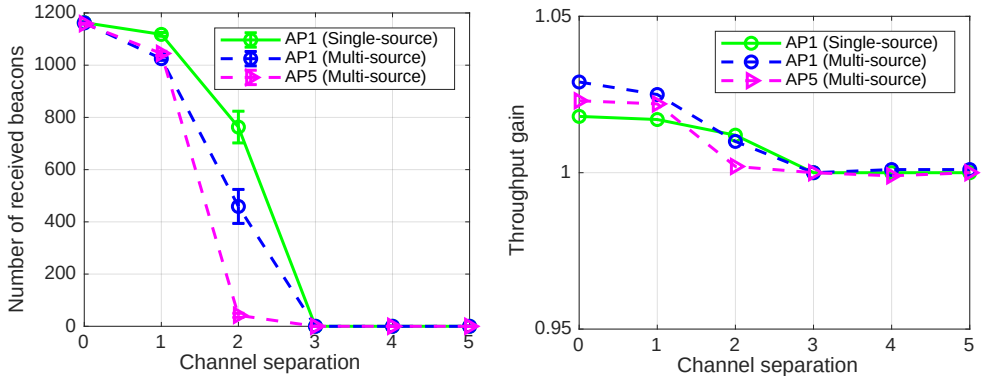

(a) Number of received beacon frames

(b) Throughput gain

Figure 2.15: Beacon riding under partially overlapped channels.

throughput of each individual AP, which depends on the locations of APs and STAs. The results are shown in Fig. 2.14. We set APs with smaller IDs as BAPs. For example, when we have 2 BAPs, AP1 and AP2 act as BAPs, and the rest as legacy APs. Interestingly, as the number of BAPs increases, the throughput performance of each AP improves. This implies that *BeaconRider* coexists well with legacy APs, and our solution not only improves the performance of BAPs but also is beneficial to legacy APs.We conjecture that riding transmissions using air-time sharing help reduce the contention overhead for typical data transmissions.

So far, we assume that all APs operate in the same channel. However, in practice, APs often operate in partially overlapped channels. Therefore, we investigate the riding performance of a BAP in partially overlapped channels. In our testbed shown in Fig. 2.9, we configure AP1 and AP5 as active, and each of which is associated with a STA. The other APs remain inactive. We let AP1 and AP5 operate in channels centered at channel j $(= 10)$ and channel k, respectively. Changing *channel separation*, i.e., the difference in channel number $|j - k|$, from 0 to 5 by setting k from 10 to 5, we count the number of received beacon frames at each AP for 2 minutes and measure the throughput gain of *BeaconRider* against the baseline. Fig. 2.15 illustrates the results.

In a single-source scenario, where only AP1 has data traffic to send, the number of

beacon frames received by AP1 decreases as the channel separation increases. When the channel separation is greater than or equal to 3, AP1 cannot receive a beacon frame from AP5. As the number of received beacon frames decreases, riding opportunities get reduced, which results in lower throughput gains as shown in Fig. 2.15(b).

In a multi-source scenario, where AP1 and AP5 have data traffic to send, we observe similar results. If their channel separation is greater than or equal to 3, they do not interfere with each other and operate independently. When their channels are partially overlapped, i.e., $|j - k| = 1$ or 2, beacon frames from the other AP may work as interference. However, our results show that a significant number of beacon frames are successfully received and they can be used to improve the performance through air-time sharing.

2.5.2 Simulation Results

To investigate the excellence of *BeaconRider* in a more dense environment, we further evaluate its performance via ns-3 simulation.

Simulation settings: We employed *Minstrel* rate adaptation algorithm as the baseline and disabled RTS/CTS for all scenarios. We assume that APs and STAs use 802.11n transmission rates, i.e., MCS 0-7, with 20 MHz bandwidth, and conform to the standard protocols. We set the transmission power of APs and STAs to 20 dBm. We set the capture threshold for the sender-last capture as 10 dB. To generate Rayleigh fading effect, the Jakes' fading model with Doppler velocity of 0.1 m/s is applied. We also apply the pathloss model in IEEE 802.11ax task group (TGax) simulation scenarios which focus on densely deployed WLANs [46]. Lastly, we set the beacon frame length and its interval to 280 bytes and default, i.e., 102.4 ms, respectively. We compare *BeaconRider* with the baseline 802.11n, and averaged the results of 100 runs for each scenario. Each run lasts for 20 s.

Topology settings: We first compare the performance of static topology scenarios for different number of BSSs, i.e., 2, 7, and 19 BSSs. Each BSS is composed of an AP

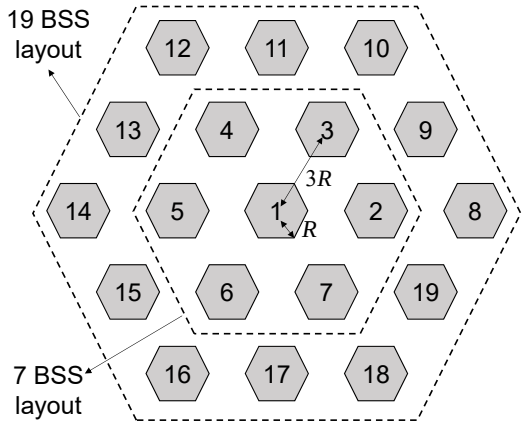

Figure 2.16: 7/19 BSS layout for a static topology scenario.

and a STA associated with it. For the case of 2 BSSs, we deploy two APs as shown in Fig. 2.5, where the distance between the two is given as 15 m. Each STA is randomly located within the radius of 5 m from its associated AP. For the case of 7 and 19 BSSs, we consider the hexagonal BSS layout of an indoor small BSS scenario in [46], which reflects high-density WLANs deployed in real environments. Assuming the frequency reuse factor of 3 is applied, we deploy 7 (19) APs from ID 1 to 7 (19) for the scenario of 7 (19) BSSs as shown in Fig. 2.16. The distance between neighboring BSSs and the coverage of each AP are given as $3R$ and R, respectively. We set $R = 5$ in all scenarios, and all APs have saturated downlink traffic destined to its associated STA.

We additionally consider the random topology of 7 and 19 BSSs. For the case of 7 (19) BSSs, we deploy BSSs randomly in a square of size 50 m $\times$ 50 m (80 m $\times$ 80 m). Each STA is randomly placed and associated with the AP with the strongest signal strength.

Results: The distribution of BRR of each STA in a static topology scenario is shown in Fig. 2.17(a). We observe that the BRR performance of *BeaconRider* slightly decreases compared with that of the baseline due to the interference from riding data transmission. Nonetheless, the degradation is very negligible and most beacon frames are well protected (i.e., the average BRRs for 2, 7, and 19 BSSs are 0.989, 0.997, and

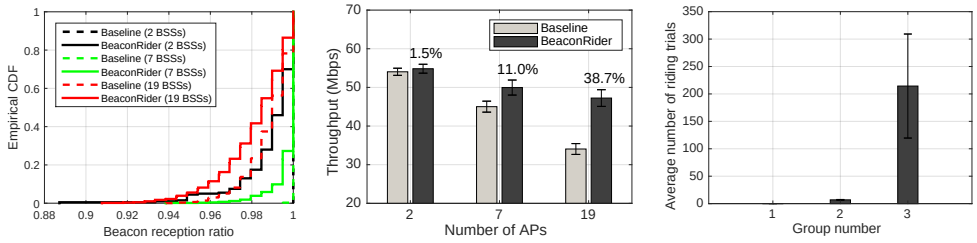

(a) Beacon reception ratio (BRR)

(b) Throughput

(c) Number of riding trials

Figure 2.17: Beacon reception ratio (BRR), throughput, and number of riding trials in a static topology scenario.

0.980, respectively). Fig. 2.17(b) shows the total network throughput according to the number of APs. As expected, due to the beacon congestion problem, the throughput of the baseline and *BeaconRider* decrease with the number of APs. Nevertheless, *BeaconRider* significantly outperforms the baseline (up to 38.7% when the number of APs is 19) thanks to extra data transmissions by beacon riding.

To further show the effectiveness of the rider selection algorithm of *BeaconRider*, we compare the average number of riding trials according to the location of each AP for the case of 19 BSSs in Fig. 2.17(c). We divide all APs into three different groups depending on the distance from the center, i.e., group 1 (AP1), group 2 (AP2-AP7), and group 3 (AP8-AP19). Since a BAP selects the AP with the lowest RSS as its rider to alleviate interference between beacon and riding data transmissions, most of riding opportunities are assigned to the APs in group 3. Accordingly, the interference between beacon and riding data transmissions can be efficiently mitigated.

Fig. 2.18(a) shows the distribution of BRR of each STA in a random topology scenario. We observe that *BeaconRider* reliably protects beacon reception at STAs with negligible reception performance degradation (i.e., the average BRRs for 7 and 19 BSSs are 0.999 and 0.983, respectively). Fig. 2.18(b) shows the total network throughput performance according to the number of APs. Again, we can see that *BeaconRider* improves performance (up to 38% when the number of deployed APs is 19) with the

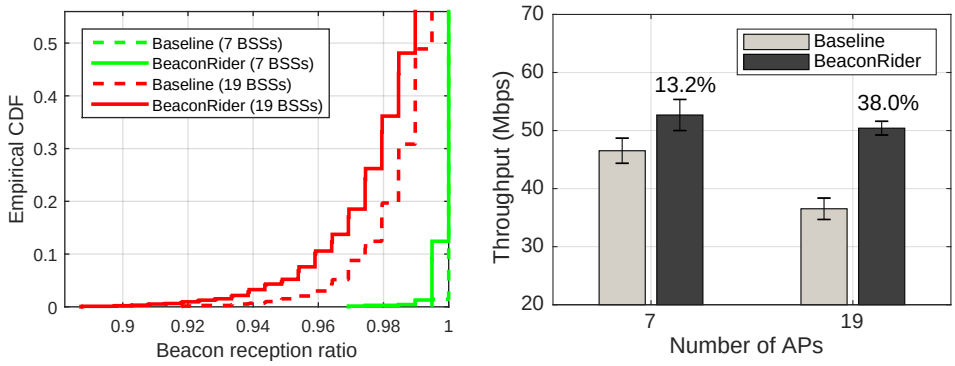

(a) Beacon reception ratio (BRR)

(b) Throughput

Figure 2.18: Beacon reception ratio (BRR) and throughput in a random topology scenario.

number of APs using additional data transmissions riding on beacon frames.

2.6 Summary

In this chapter, we addressed the beacon congestion problem and developed an opportunistic air-time sharing scheme, named *BeaconRider*, that *rides* on beacon air-time by exploiting the capture effect. *BeaconRider* is backward compatible and coordinates with each other in a distributed manner without incurring additional control message exchange. Our extensive experiments and simulations showed that *BeaconRider* achieves significant performance gains that increase linearly with the number of participating APs.

Our approach may be extended to transmission of other control, management, and low-rate data frames. For example, probe response frames used to discover 802.11 networks are transmitted at the lowest transmission rate. They can reduce available air-time further in high-density WLANs [47, 48]. Our riding technique can be applied on the probe response frames, which remains as an interesting future work.

Chapter 3

OSR: Opportunistic Spatial Reuse in IEEE 802.11ax WLANs

3.1 Introduction

With the exponential growth of mobile devices, demands for wireless traffic and quality of service (QoS) have dramatically increased in recent years. Wireless local area networks (WLANs) have attracted great attention for supporting the traffic demands due to the its high speed, ease of deployment, and low cost.

The increasing popularity of WLANs in the last decades has led to a massive deployment of access points (APs) and stations (STAs) in residential areas such as apartments, offices, and campus buildings. As a result, it is becoming easy to find multiple overlapping basic service sets (OBSSs) coexist in limited geographical areas. However, the unplanned and unmanaged BSS deployment exacerbates network performance due to the interference between neighboring BSSs.

To address the issues and challenges in dense environments, the IEEE 802.11ax task group (TGax) is currently developing next generation WLAN standard aiming for high efficiency WLANs (HEW). The goal of IEEE 802.11ax are to not only improve the overall system throughput but also the average per-STA throughput by four times. To this end, it includes several new technical features such as orthogonal frequency-division multiple access (OFDMA), downlink/uplink multi-user MIMO (DL/UL MU-

MIMO), power saving with target wake time (TWT), and spatial reuse (SR) operation.

In this chapter, we focus on the SR operation of 802.11ax, which aims to increase the number of simultaneous transmissions. To achieve this, 802.11ax introduces OBSS packet detection (OBSS PD)-based SR which uses both carrier sensing threshold (CST) adjustment and transmission power control (TPC) for the OBSS transmissions. Specifically, when using OBSS PD-based SR, an HE AP/STA may ignore ongoing OBSS transmissions if the received signal strength (RSS) is lower than the OBSS PD level and initialize its own transmissions in conjunction with reduced transmission power. However, OBSS PD-based SR operation has intrinsic limitations because it does not consider the impact of the SR transmissions on the receiver of the ongoing transmissions.

To overcome the limitations, we propose an opportunistic spatial reuse scheme called *OSR* that allows simultaneous data transmissions during the ongoing transmissions of neighboring BSSs. *OSR* selects two appropriate APs such that the ongoing data transmission is sufficiently protected from the interference of the SR data-ACK transmissions, and increases the SR throughput improvement by opportunistically selecting SR link and modulation coding scheme (MCS). To prevent from incurring additional control overhead, *OSR* reuses BSS color field and reserved 3 bits in HE preamble for operations. Our goal is to fully utilize SR opportunity by opportunistically engaging in simultaneous data transmissions. To this end, we develop a distributed protocol that coordinates SR operation in an efficient and reliable manner.

Our main contributions are as follows.

- We introduce OBSS PD-based SR operation proposed in 802.11ax and investigate its own limitations.
- We develop an opportunistic spatial reuse scheme, *OSR*, that allows simultaneous data transmission during the ongoing transmission of neighboring BSSs. The proposed method provides distributed coordination between APs without

incurring additional control message exchange.

- Through extensive simulation using ns-3 [33] under a variety of network environments, we demonstrate that *OSR* significantly improves throughput performance.

The rest of this chapter is organized as follows. In Section 3.2, we introduce OBSS PD-based SR operation and describe its limitations. Section 3.3 presents a detailed design of *OSR*. We evaluate the performance of *OSR* via ns-3 simulation in Section 3.4. Finally, we summarize this chapter in Section 3.5.

3.2 OBSS PD-based Spatial Reuse

3.2.1 Procedures

The goal of HE SR operation is to allow the medium to be reused by multiple BSSs in dense deployment by early identification of transmission from OBSSs. To this end, IEEE 802.11ax amendment introduces OBSS packet detection (OBSS PD)-based SR operation.

The OBSS PD-based SR operation is based on the adjustment of the CST and TPC jointly to cope with the OBSS interference. Upon detecting an ongoing transmission, an HE AP/STA determine whether the frame is intra-BSS frame or inter-BSS frame based on the BSS color field in the HE preamble. If the frame comes from OBSS, the AP/STA applies different CST called OBSS PD threshold (i.e., $OBSS_PD_{\mathrm{th}}$). If the RSS of ongoing transmission is below this threshold, the HE AP/STA initializes SR transmissions, thus improving channel utilization. The $OBSS_PD_{\mathrm{th}}$ is given as

$$\begin{aligned} OBSS_PD_{\mathrm{max}} \leq & max(OBSS_PD_{\mathrm{min}}, \\ & min\left(OBSS_PD_{\mathrm{max}}, OBSS_PD_{\mathrm{min}} + (TX_PWR_{\mathrm{ref}} - TX_PWR)\right), \end{aligned}$$

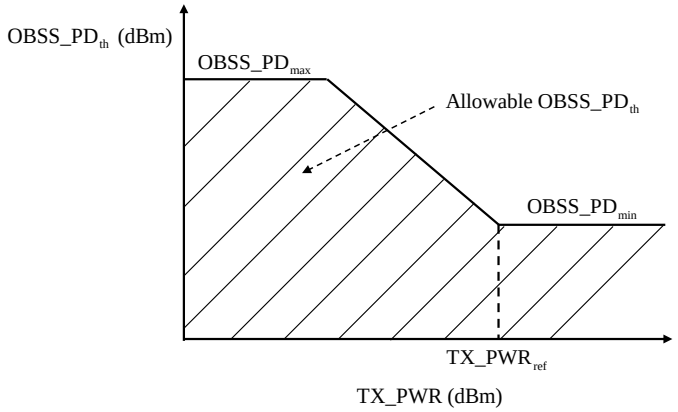

Figure 3.1: Illustration of the adjustment of OBSS PD threshold.

where $OBSS_PD_{\min}$ and $OBSS_PD_{\max}$ are set to -82 dBm and -62 dBm, respectively. The reference power TX_PWR_{ref} is set to 21 dBm by default, and TX_PWR is the transmission power of SR transmission. This adjustment is illustrated in Fig. 3.1.

If an HE AP/STA selects a certain OBSS PD threshold, the maximum transmission power for SR transmission is given as

$$TX_PWR_{\max} = TX_PWR_{\text{ref}} - (OBSS_PD_{\text{th}} - OBSS_PD_{\min}). \quad (3.1)$$

Therefore, the higher OBSS PD threshold is selected, the more transmission power should be reduced. By doing this, the impact of interference from SR transmission on the ongoing transmission can be mitigated. Note that the power restriction period ends at the end of the SR opportunity.

3.2.2 Limitations

The main drawback of OBSS PD-based SR operation is that it initiates SR transmission based on the RSS of ongoing transmission. Although OBSS PD-based SR operation reduces SR transmission power to reduce the impact of interference to ongoing transmissions, SR transmitter can not precisely predict the reception of the ongoing transmission at the receiver. We summarize major limitations of OBSS PD-based SR operation as follows.

- Underutilization of SR opportunity: If the RSS of received OBSS frame is higher than OBSS PD threshold, an HE AP/STA does not trigger SR transmission. As a result, SR opportunity may be underutilized when transmitters are closely located each other while receivers are located far enough. (i.e., exposed node problem).

- Aggressive SR: On the contrary, if the transmitters are closely located each other while receivers are located between the transmitter, SR transmitter may aggressively initiates its SR transmission without considering the interference from ongoing transmission to its own receiver. In this case, the SR opportunity can be wasted without channel utilization gain.

- No protection for ongoing transmission: Since SR transmitter initiates its SR transmission when the RSS of the ongoing transmission is below the OBSS PD threshold, it may hinder the reception of ongoing transmission receiver. For example, if the receiver of ongoing transmission is located closely to the SR transmitter, the frame errors can occur even with the reduced SR transmission power.

- No MCS control for SR transmission: In OBSS PD-based SR operation, selecting MCS for SR transmission is not defined and left open to implementation and vendors. Therefore, appropriate MCS selection algorithm is also needed.

3.3 Design of *OSR*

In this section, we propose *OSR*, an opportunistic spatial reuse scheme that allows SR transmission while protecting ongoing transmission by transmission power control. We first provide the overview of *OSR*, and explain its operation in detail.

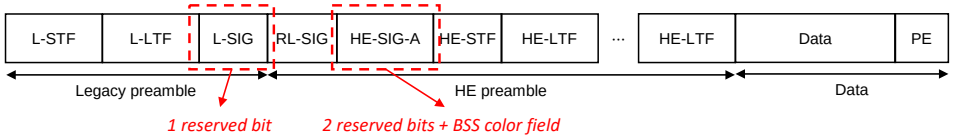

Figure 3.2: HE PPDU frame format.

3.3.1 Overview of *OSR*

To avoid additional control message exchange for the coordination, we reuse *BSS color* field and reserved 3 bits in legacy and HE preamble as marked in Fig. 3.2. The control information used in *OSR* operations are summarized as follows.

- OBSS link (i.e, OBSS color and OBSS receiver (RX) link ID)
- SR scheduled BSS Color
- SR TPC request for SR BSS
- *OSR* node indicator
- Buffer status of *OSR* node

We explain the overall operation through the following three actions.

1. **Listening:** A OSR node listens to data frames from neighboring BSSs, and collects information needed to determine whether the neighbor node is OSR node or not. Based on the buffer status of the OSR node, it also confirm if it needs SR opportunity. Using the information, it schedules one of neighboring BSSs needs SR opportunity to initialize its SR transmission with ongoing transmission. The selection may change over time according to the channel state.

2. **Informing SR BSS selection:** When transmitting data frames, each OSR node informs its neighboring BSSs of the latest decision on scheduled BSS through using the BSS color field of the data frame.

3. **SR transmission:** An OSR node first obtains link information of the ongoing transmission after receiving RTS frame. Then, while receiving a following data frame, the OSR node quickly checks the BSS color field in the HE-SIG-A field in the data frame. If the BSS color is matched with its own BSS color, it immediately stops receiving the data frame and starts SR transmission with restricted transmission power.

3.3.2 Listening

The important task of the ongoing transmitter is to select the right SR transmitter, enabled to use SR opportunity. The ongoing and SR transmissions should not interfere with each other. Moreover, BSS coordination should proceed without a central entity or additional control message exchange, conforming to the distributed nature of the WLAN protocol and backward compatibility.

In our scheme, the OSR node continues listening to data frames from its neighboring BSSs, and collecting the information of received signal strength (RSS), buffer status, and OSR node indication. If the data frame is transmitted from an OSR node, it computes average RSS through exponential weighted moving average (EWMA). By default, we set the weight factor of EWMA to 0.125.

3.3.3 SR BSS Selection

At every data transmission, the OSR nodes selects the BSS color with the lowest average RSS among the list of neighboring BSSs with non-empty buffer, and allows the BSS to utilize the SR opportunity. The OSR node informs neighboring BSSs of the decision on SR BSS scheduling by setting the BSS color field of the data frame to the BSS color of the target BSS. If the previously scheduled SR transmission interfered with the ongoing transmission, the OSR node also sets the SR TPC request bit to 1 to indicate the SR scheduled BSS to reduce its transmission power.

3.3.4 SR Transmission

Upon receiving a data frame, the OSR node begins to decode its BSS color field. If the BSS color in the BSS color field matches with its own BSS color, the OSR node initialize its SR transmission, i.e., immediately stops receiving the data frame and starts to transmit a data frame.

Note that the ongoing transmission is protected from the interference of SR transmission through TPC request. If the transmission power of SR transmission is too strong, the OSR node of ongoing transmission will notify the OSR node of SR transmission to reduce transmission power. If it is not, the OSR node for SR transmission will use the same transmission power for its SR transmission. To further protect the ACK reception of ongoing transmission, OSR node of SR transmission controls the length of the SR data frame by aggregating several subframes such that the transmission of aggregated SR data frame lasts shorter than the ongoing data transmission, which ensures no transmission overlap between the SR data/ACK frames and the block ACK (BlockACK) frame paired with the ongoing data frame.

On the other hand, the data reception from SR transmission may not be protected from the interference of ongoing transmission if the sender of ongoing transmission is close to the SR transmission receiver. To address these problems, we carefully choose the MCS level, and the final decision on a SR transmission.

MCS selection

Another important decision that the OSR node of SR transmission should make is about the MCS level for data frame transmission. From the viewpoint of the receiver of the SR data frame, ongoing data transmission appears as interference. As a result, the OSR node may need to lower its MCS level than usual.

To find the right MCS level, we define a expected SR gain for each MCS level x and SR receiver k using subframe error rate (SFER), i.e., $\tilde{e}_{k,x}$. The expected SR gain

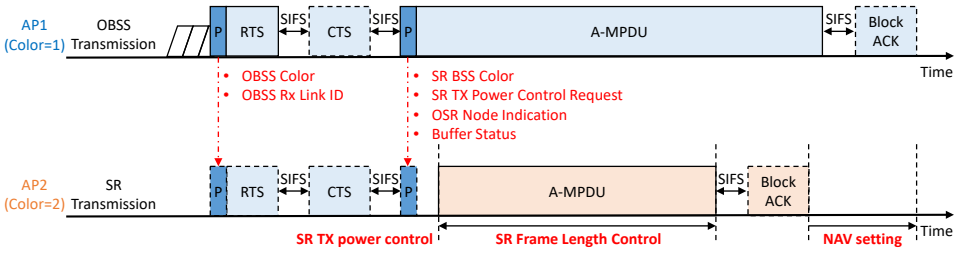

Figure 3.3: Timeline example of OSR transmission.

$G_{k,x}$ of MCS x given k is updated as

$$G_{k,x} = r_x \cdot (1 - \tilde{e}_{k,x}) \cdot t^x_{\mathrm{SR}}, \tag{3.2}$$

where r_x denotes the transmission rate under MCS x, and t^x_{SR} denotes the SR transmission duration under MCS x, as shown in Fig. 3.3. The OSR nodes chooses the MCS level x^* with the highest expected gain, i.e., $x^* = \arg\max_x G_{k,x}$. We break a tie arbitrarily.

3.4 Performance Evaluation

In this section, we evaluate the performance of *OSR* through extensive simulations with ns-3.

3.4.1 Simulation Setup

We employed *Minstrel* rate adaptation algorithm as the baseline for all scenarios. We assume that APs and STAs use 802.11n transmission rates, i.e., MCS 0-7, with 20 MHz bandwidth, and conform to the standard protocols. We set the transmission power of APs and STAs to 20 dBm and 15 dBm, respectively. We set the capture threshold for the sender-last capture as 10 dB. To generate Rayleigh fading effect, the Jakes' fading model with Doppler velocity of 0.1 m/s is applied. We also apply the pathloss model in IEEE 802.11ax task group (TGax) simulation scenarios which focus on densely

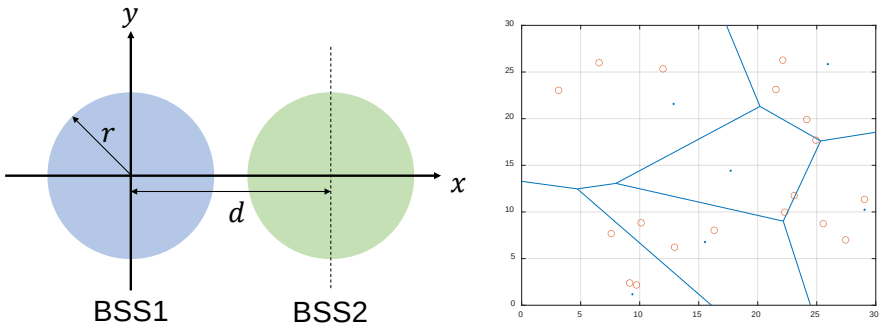

(a) 2 BSS layout for a static topology scenario (b) 6 BSS layout for a random topology scenario

Figure 3.4: BSS layout for simulation topology.

deployed WLANs [46]. We compare *OSR* with the baseline 802.11n and OBSS PD-based SR, and averaged the results of 100 runs for each scenario. Each run lasts for 5 s.

Topology settings: We first compare the performance of static topology scenarios of 2 BSSs for different inter BSS distance, i.e., 10, 20, 30, 40, and 50 m. Each BSS is composed of an AP and 1-5 STAs associated with it. Each STA is randomly located within the radius of 10 m from its associated AP.

We additionally consider the random topology of 2, 4, 6, 8, 10 BSSs. We deploy BSSs randomly in a square of size 30 m $\times$ 30 m. Each STA is randomly placed and associated with the AP with the strongest signal strength with maximum distance of 10 m.

3.4.2 Simulation Results

The per-BSS average throughput according to the inter BSS distance is shown in Fig. 3.5. We first observe that the throughput performance of all compared schemes shows similar when the inter BSS distance is very close, i.e, 10m. In this case, OBSS PD does not perform SR transmission because the RSS from ongoing transmission is mostly higher than the maximum OBSS PD threshold, i.e., -62 dBm. Meanwhile, OSR initializes its SR transmission in its initial phase but to find out that there is no feasible

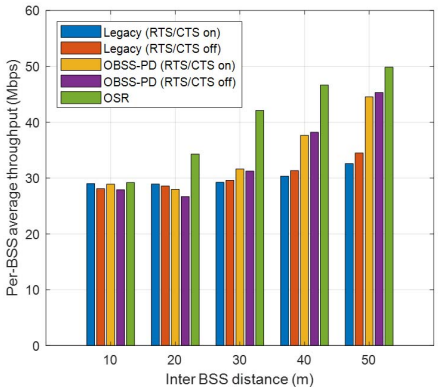

Figure 3.5: Throughput for a two BSSs scenario.

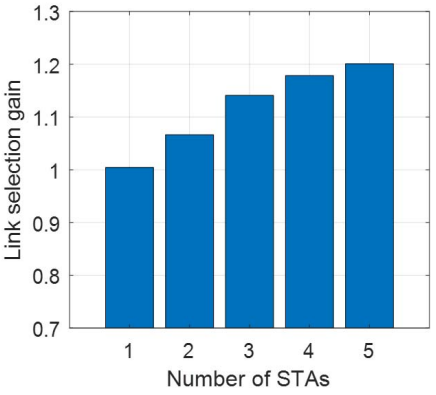

Figure 3.6: Link selection gain for a two BSSs scenario.

SR transmission link and finally stops trying SR transmission. On the other hand, as the inter BSS distance increases, both OBSS PD ans OSR outperforms legacy 802.11n by utilizing SR opportunity. We can also confirm that OSR outperforms OBSS PD since OSR adaptively selects SR transmission link and MCS for better reliability.

To show the effectiveness of the link selection algorithm of *OSR*, we compare the throughput gain of OSR with link selection over OSR without link selection according to the number of STAs in Fig. 3.6. Since a OSR AP selects the STA suffering from the lowest interference from ongoing transmission as its SR transmission receiver, the SR opportunity can be reliably utilized. As a result, the link selection gain increases

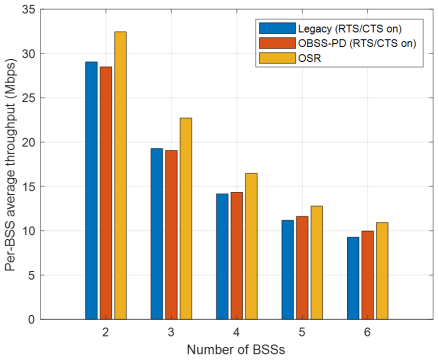

Figure 3.7: Throughput for a multiple BSSs scenario.

linearly with the number of associated STAs.

Lastly, we compare the throughput of all comparing schemes in random topology scenario in Fig. 3.7. We can observe that OSR outperforms both legacy and OBSS PD for the different number of BSSs.

3.5 Summary

In this chapter, we focused on SR operation proposed in 802.11ax standard and developed an opportunistic spatial reuse scheme, named *OSR*, that opportunistically initiates SR transmission depending on the ongoing link and allowed SR transmission power. *OSR* coordinates with each other in a distributed manner without incurring additional control message exchange. Our simulation results showed that *OSR* achieves significant performance gains with link selection and MCS control for SR transmission.

Chapter 4

Conclusion

In this dissertation, we proposed opportunistic spatial reuse algorithms that improves network throughput in high-density WLANs.

First, we addressed the beacon congestion problem and developed an opportunistic air-time sharing scheme, named *BeaconRider*, that *rides* on beacon air-time by exploiting the capture effect. The protocol selects two appropriate APs such that the beacon frame is sufficiently protected from the interference of the data-ACK transmissions, and at the same time, data-ACK transmissions are likely to be successful under beacon interference. *BeaconRider* is backward compatible and coordinates with each other in a distributed manner without incurring additional control message exchange. Our extensive experiments and simulations showed that *BeaconRider* achieves significant performance gains that increase linearly with the number of participating APs.

Secondly, we have developed an opportunistic spatial reuse scheme called *OSR* that allows simultaneous data transmissions during the ongoing transmissions of neighboring BSSs. *OSR* selects two appropriate APs such that the ongoing data transmission is sufficiently protected from the interference of the SR data-ACK transmissions, and increases the SR throughput improvement by opportunistically selecting SR link and modulation coding scheme (MCS). To prevent from incurring additional control overhead, *OSR* reuses BSS color field and reserved 3 bits in HE preamble for operations.

Our goal is to fully utilize SR opportunity by opportunistically engaging in simultaneous data transmissions. To this end, we develop a distributed protocol that coordinates SR operation in an efficient and reliable manner.

To summarize, this dissertation sheds light on SR operations for improving network throughput in high-density WLANs. Since there still remain many issues and many interesting problems to resolve, we hope this dissertation can be a guideline for future researchers.

Bibliography

[1] B. Bellalta, "IEEE 802.11ax: high-efficiency WLANs," *IEEE Wireless Communications*, vol. 23, no. 1, pp. 38–46, Feb. 2016.

[2] D.-J. Deng, Y.-P. Lin, X. Yang, J. Zhu, Y.-B. Li, J. Luo, and K.-C. Chen, "IEEE 802.11ax: highly efficient WLANs for intelligent information infrastructure," *IEEE Communications Magazine*, vol. 55, no. 12, pp. 52–59, Dec. 2017.

[3] E. Khorov, A. Kiryanov, A. Lyakhov, and G. Bianchi, "A tutorial on IEEE 802.11ax high efficiency WLANs," *IEEE Communications Surveys and Tutorials*, vol. 21, no. 1, pp. 197–216, Sep. 2018.

[4] A. Kochut, A. Vasan, A. U. Shankar, and A. Agrawala, "Sniffing out the correct physical layer capture model in 802.11b," in *Proc. IEEE ICNP*, Nov. 2004.

[5] J. Manweiler, N. Santhapuri, S. Sen, R. R. Choudhury, S. Nelakuditi, and K. Munagala, "Order matters: Transmission reordering in wireless networks," *IEEE/ACM Trans. on Networking*, vol. 20, no. 2, pp. 353–366, Apr. 2012.

[6] J.-W. Dai, "The system performance of wireless CSMA/CA protocol with capture effect," *KICS Journal of Communications and Networks*, vol. 6, no. 3, pp. 226–234, Sep. 2004.

[7] J. Lee *et al.*, "An experimental study on the capture effect in 802.11a networks," in *Proc. ACM WiNTECH*, Sep. 2007.

[8] S. Sati and K. Graffi, "Adapting the beacon interval for opportunistic network communications," in *Proc. IEEE ICACCI*, Aug. 2015.

[9] S. Nath, Z. Anderson, and S. Seshan, "Choosing beacon periods to improve response times for wireless HTTP clients," in *Proc. ACM MobiWac*, Oct. 2004.

[10] Y. Xie, X. Luo, and R. K. Chang, "Centralized PSM: an AP-centric power saving mode for 802.11 infrastructure networks," in *Proc. IEEE SARNOFF*, Mar. 2009.

[11] L. Le, R. Baldessari, P. Salvador, A. Festag, and W. Zhang, "Performance evaluation of beacon congestion control algorithms for VANETs," in *Proc. IEEE GlobeCom*, Dec. 2011.

[12] S. Bolufé *et al.*, "Dynamic control of beacon transmission rate and power with position error constraint in cooperative vehicular networks," in *Proc. ACM SAC*, Apr. 2018.

[13] Y. Mo, D. Yu, J. Song, K. Zheng, and Y. Guo, "A beacon transmission power control algorithm based on wireless channel load forecasting in VANETs," *PloS one*, vol. 10, no. 11, pp. 1–17, Nov. 2015.

[14] M. Torrent-Moreno, P. Santi, and H. Hartenstein, "Distributed fair transmit power adjustment for vehicular ad hoc networks," in *Proc. IEEE SECON*, Sep. 2006.

[15] G. Caizzone, P. Giacomazzi, L. Musumeci, and G. Verticale, "A power control algorithm with high channel availability for vehicular ad hoc networks," in *Proc. IEEE ICC*, May 2005.

[16] V. Shrivastava, N. Ahmed, S. Rayanchu, S. Banerjee, S. Keshav, K. Papagiannaki, and A. Mishra, "CENTAUR: realizing the full potential of centralized WLANs through a hybrid data path," in *Proc. ACM MobiCom*, Sep. 2009.

[17] M. Vutukuru, K. Jamieson, and H. Balakrishnan, "Harnessing exposed terminals in wireless networks," in *Proc. USENIX NSDI*, Apr. 2008.

[18] Y. Kang, J. Yoo, J. Lee, and C. Kim, "A distributed message in message aware concurrent transmission protocol in IEEE 802.11 WLANs," *EURASIP Journal on Wireless Communications and Networking*, vol. 1, no. 325, Oct. 2012.

[19] S. Katti, S. Gollakota, and D. Katabi, "Embracing wireless interference: Analog network coding," in *Proc. ACM SIGCOMM*, Aug. 2007.

[20] S. Gollakota and D. Katabi, "Zigzag decoding: combating hidden terminals in wireless networks," in *Proc. ACM SIGCOMM*, Aug. 2008.

[21] S. Gollakota, S. D. Perli, and D. Katabi, "Interference alignment and cancellation," in *Proc. ACM SIGCOMM*, Aug. 2009.

[22] J. Han, C. Joo, and S. Bahk, "Resource sharing in dual-stack devices: Opportunistic bluetooth transmissions in WLAN busy periods," *IEEE Trans. on Mobile Computing*, vol. 17, no. 10, pp. 2396–2407, Oct. 2018.

[23] W. Park, J. Han, S. Jang, and S. Bahk, "OAU: Opportunistic antenna utilization for Wi-Fi and bluetooth coexistence," in *Proc. IEEE GlobeCom*, Dec. 2016.

[24] G. Smith, "Dynamic sensitivity control-v2," *IEEE*, vol. 802, pp. 802–11, 2013.

[25] M. S. Afaqui, E. Garcia-Villegas, E. Lopez-Aguilera, G. Smith, and D. Camps, "Evaluation of dynamic sensitivity control algorithm for IEEE 802.11 ax," in *Proc. IEEE WCNC*, May 2015.

[26] M. S. Afaqui, E. Garcia-Villegas, E. Lopez-Aguilera, and D. Camps-Mur, "Dynamic sensitivity control of access points for IEEE 802.11ax," in *Proc. IEEE ICC*, May 2016.

[27] I. Selinis, K. Katsaros, S. Vahid, and R. Tafazolli, "Control OBSS/PD sensitivity threshold for IEEE 802.11ax BSS color," in *Proc. IEEE PIMRC*, Sep. 2018.

[28] T. Ropitault, "Evaluation of RTOT algorithm: A first implementation of OBSS_PD-based SR method for IEEE 802.11 ax," in *Proc. IEEE CCNC*, Jan 2018.

[29] Cisco visual networking index, "Global mobile data traffic forecast update, 2016–2021," Feb. 2017.

[30] IEEE 802.11, *Part 11: Wireless LAN medium access control (MAC) and physical layer (PHY) specifications*, IEEE Std., Mar. 2012.

[31] IEEE 802.11ac, *Part 11: Wireless LAN medium access control (MAC) and physical layer (PHY) specifications: Enhancements for very high throughput for operation in bands below 6 GHz*, IEEE Std., Dec. 2013.

[32] Ath9k-htc: Atheros wireless device firmware. https://github.com/qca/open-ath9k-htc-firmware.

[33] The network simulator 3 – *ns*-3. http://www.nsnam.org/.

[34] A. Farshad, M. K. Marina, and F. Garcia, "Urban WiFi characterization via mobile crowdsensing," in *Proc. IEEE NOMS*, May 2014.

[35] S. Biswas, J. Bicket, E. Wong, R. Musaloiu-e, A. Bhartia, and D. Aguayo, "Large-scale measurements of wireless network behavior," in *ACM SIGCOMM*, Aug. 2015.

[36] K. Sui, M. Zhou, D. Liu, M. Ma, D. Pei, Y. Zhao, Z. Li, and T. Moscibroda, "Characterizing and improving WiFi latency in large-scale operational networks," in *Proc. ACM MobiSys*, Jun. 2016.

[37] Wireshark 2.2.3. https://www.wireshark.org/.

[38] J. Yi, W. Sun, J. Koo, S. Byeon, J. Choi, and S. Choi, "BlueScan: Boosting Wi-Fi scanning efficiency using bluetooth radio," in *Proc. IEEE SECON*, Jun. 2018.

[39] Android open source project. https://source.android.com/.

[40] S. Kim, J. Yi, Y. Son, S. Yoo, and S. Choi, "Quiet ACK: ACK transmit power control in IEEE 802.11 WLANs," in *Proc. IEEE INFOCOM*, Apr. 2017.

[41] N. Kanirkar and J. Sarvaiya, "BER Vs SNR performance comparison of DSSS-CDMA FPGA based hardware with AWGN, spreading codes & code modulation techniques," *International Journal of Electronic Engineering Research*, vol. 1, no. 2, pp. 155–168, 2009.

[42] G. Pei and T. Henderson, "Validation of ns-3 802.11b PHY model," *http://www.nsnam.org/p̃ei/80211b.pdf*, May 2009.

[43] *BeaconRider* source code. https://github.com/makesens86/BeaconRider.

[44] M. Vanhoef and F. Piessens, "Advanced Wi-Fi attacks using commodity hardware," in *Proc. ACM ACSAC*, Dec. 2014.

[45] Hostapd: IEEE 802.11 AP, IEEE 802.1X, WPA/WPA2/EAP/RADIUS Authenticator. https://w1.fi/hostapd/.

[46] IEEE P802.11, *TGax simulation scenarios*, Jul. 2015.

[47] R. Raghavendra, E. M. Belding, K. Papagiannaki, and K. C. Almeroth, "Unwanted link layer traffic in large IEEE 802.11 wireless networks," *IEEE Trans. on Mobile Computing*, vol. 9, no. 9, pp. 1212–1225, Sep. 2010.

[48] X. Hu, L. Song, D. Van Bruggen, and A. Striegel, "Is there WiFi yet?: How aggressive probe requests deteriorate energy and throughput," in *Proc. ACM IMC*, Oct. 2015.

초 록

최근 들어 모바일 트래픽의 양이 급증함에 따라 IEEE 802.11 기능을 지원하는 무선랜 환경이 조밀 조밀하게 배치되기 시작하였다. 그 결과, 인접한 basic service sets (BSSs) 에서 미치는 간섭 효과로 인하여, 데이터 전송을 위한 전송 시간이 급격히 줄어드는 문제가 발생하였다. 본 논문에서는 이러한 간섭으로 인한 데이터 전송 기회 감소 문제를 해결하고 효과적인 동시 전송을 활용하여 네트워크의 수율을 높이는 기법들을 제안한다.

첫째, 많은 수의 무선랜이 밀집되어 분포된 환경에서는 공유기가 전송하는 비콘 프레임으로 인해 데이터를 전송할 수 있는 시간이 줄어들게 되는데, 이러한 비콘으로 인한 전송 시간 부족 문제를 해결하기 위해서 비콘 프레임과 데이터 프레임의 전송 시간 공유 기법인 BeaconRider를 제안하였다. 제안 기법은 하향 링크를 가정하고 있으며, 여러 개의 공유기들은 프레임 캡쳐 효과를 활용한 전송 기회를 이용하기 위해서 주변의 공유기들과 분산적으로 동작을 조율한다. 제안 기법은 해당 제안 기법을 탑재하지 않은 기존의 공유기들과 공존 할 수 있다는 장점이 있다. 제안 기법의 성능을 평가하기 위해서 제안 기법을 실제 상용 무선랜 동글에 구현하였으며, 추가로 ns-3 시뮬레이션을 진행하였다. 실험 결과와 시뮬레이션을 통해서 제안기법이 기존 기법 대비 월등한 수율을 얻을 수 있었고, 수율의 비율은 배치된 공유기의 개수에 비례함을 확인하였다.

둘째, 인접한 BSS 간의 거리가 가까워질수록 주변에 미치는 간섭 효과 때문에 발생 할 수 있는 데이터 전송 기회 부족 문제를 해결하기 위해서, 동시에 데이터 전송을 가능하게 함으로써 밀집된 환경에서 동시 전송 기회를 활용하는 OSR을 제안

하였다. 제안 기법은 무선랜의 새로운 표준인 IEEE 802.11ax 네트워크에서의 하향 링크 상황을 가정하였다. 제안 기법은 여러 개의 공유기들의 정보 교환에 필요한 추가적인 오버헤드 발생 없이 분산적으로 동작하면서 동시 전송 기회를 효과적으로 얻는다. ns-3 시뮬레이션을 통해서 제안기법이 동시 전송 링크를 효과적으로 선택함으로써 기존 기법 대비 네트워크의 수율을 월등히 향상하는 것을 확인하였다.

주요어: 비콘, 전송 시간 공유, 캡쳐 효과, 공간 재사용, 고밀도 무선랜
학번: 2012-20846